Seasonal dependency of the atmospheric oxidizing capacity of the marine boundary layer of Bermuda

Yasin Elshorbany, Yuting Zhu, Youfeng Wang, Xianliang Zhou, Summer Sanderfield, Chunxiang Ye, Matthew Hayden, Andrew J. Peters

ATMOSPHERIC ENVIRONMENT

PII: \$1352-2310(22)00391-0

DOI: https://doi.org/10.1016/j.atmosenv.2022.119326

Reference: AEA 119326

To appear in: Atmospheric Environment

Received Date: 8 April 2022
Revised Date: 28 June 2022
Accepted Date: 4 August 2022

Please cite this article as: Elshorbany, Y., Zhu, Y., Wang, Y., Zhou, X., Sanderfield, S., Ye, C., Hayden, M., Peters, A.J., Seasonal dependency of the atmospheric oxidizing capacity of the marine boundary layer of Bermuda, *Atmospheric Environment* (2022), doi: https://doi.org/10.1016/j.atmosenv.2022.119326.

This is a PDF file of an article that has undergone enhancements after acceptance, such as the addition of a cover page and metadata, and formatting for readability, but it is not yet the definitive version of record. This version will undergo additional copyediting, typesetting and review before it is published in its final form, but we are providing this version to give early visibility of the article. Please note that, during the production process, errors may be discovered which could affect the content, and all legal disclaimers that apply to the journal pertain.

© 2022 Published by Elsevier Ltd.

Credit Statement

Yasin Elshorbany: conceptualization, measurements, model simulations, data analysis, writing

Yuting Zhu: measurements, data analysis, writing

Youfeng Wang: measurements, data analysis, writing

Xianliang Zhou: measurements, data analysis, writing

Summer Sanderfield: model simulations, data analysis, writing

Chunxiang Ye: measurements, data analysis

Matthew Hayden: data analysis, writing

Andrew J. Peters: measurements

Seasonal Dependency of the Atmospheric Oxidizing Capacity of the Marine Boundary Layer of Bermuda

Yasin Elshorbany^{1*}, Yuting Zhu^{2,3}, Youfeng Wang^{2,4}, Xianliang Zhou^{2,5}, Summer Sanderfield¹, Chunxiang Ye⁴, Matthew Hayden⁶, Andrew J. Peters⁶

¹College of Arts and Sciences, University of South Florida, St. Petersburg, FL, United States

²Wadsworth Center, New York State Department of Health, Albany, NY, United States

³Now at: Department of Marine Chemistry and Geochemistry, Woods Hole Oceanographic Institution, Woods Hole, Massachusetts, United States

⁴College of Environmental Sciences and Engineering, State Key Laboratory of Environmental Simulation and Pollution Control, Peking University, Beijing, China

⁵Department of Environmental Health Sciences, University at Albany, SUNY, Albany, United States

⁶Bermuda Institute of Ocean Sciences, St. George's, Bermuda

*Corresponding author: elshorbany@usf.edu

Abstract

5

10

15

20

25

30

In this study, we investigate the atmospheric oxidation capacity in the marine boundary layer during two measurement campaigns in spring and summer 2019 at the Tudor Hill Marine Atmospheric Observatory, Bermuda. Measured species included non-methane hydrocarbons (NMHCs), HONO, HNO₃, particulate matter, particulate nitrates, NO, NO₂, O₃, in addition to the meteorological parameters. Measured concentrations of all species were generally higher in spring than in summer. During the spring and summer, OH initiation sources made 61% and 42% of the total OH production rate (PoH) during the daytime, respectively. The higher levels of NMHCs and OH production from ozone photolysis lead to a higher oxidation rate of NMHCs in the spring compared to summer. However, the low NO in the spring and summer leads to inefficient recycling of RO₂ and HO₂ to OH with HO₂ reaction with NO accounting for only 22% and 42% of PoH during spring and summer. Sensitivity analysis suggests that OH reactivity in the MBL can be potentially enhanced by an oceanic source rather than a secondary oxidation product. Including halogen monoxides, BrO and IO were found to decrease HO₂ by ~14 and 18% during spring and summer, respectively, with marginal impact on OH due to the higher loss by aerosol uptake. The results demonstrate the complex multiphase HOx-Halogen chemistry and call for a more comprehensive multiphase investigation.

35 Keywords: Marine Boundary Layer, NO_x-limited Conditions, HO_x budget, Oxidation Capacity

1. Introduction

40

45

50

55

60

65

70

75

80

The atmospheric oxidizing capacity describes the rate of removal and abundance of air pollutants (e.g., carbon monoxide (CO), methane, and non-methane hydrocarbons (NMHCs)) in the atmosphere (e.g., Prinn, 2003; Elshorbany et al., 2009a). However, the oxidation mechanisms by which these species are degraded in the atmosphere result in the formation of other harmful species (e.g., ozone (O₃) and peroxyl acyl nitrates (PAN)). Therefore, understanding the processes and rates by which trace gases are oxidized in the atmosphere is paramount to our knowledge of the atmospheric composition and climate. The term "oxidation capacity", OC is the sum of the respective oxidation rates of the molecules Y_i (VOCs, CO, CH₄) by the oxidant X (X=OH, O₃, NO₃) (Geyer et al., 2001), OC= Σ ky_i[Y_i][X], where ky_i is the bi-molecular rate constant for the reaction of Y_i with X. OH is the dominant oxidizing species, responsible for the degradation of most trace gasses (e.g., Elshorbany et al., 2010b; Carpenter et al, 2010). The effectiveness of the OH removal of species Y can be calculated from the OH reactivity, the inverse of OH lifetime.

The atmospheric marine boundary layer (MBL) is where the ocean and atmosphere exchange heat, moisture, and energy (Fairall et al., 1996) but also chemical constituents (e.g., Van Den Berg et al., 2000; Br ggemann et al., 2018). Recent studies showed that oceans can be a sink or a source of several volatile organic compounds (VOCs) (e.g., Coburn et al., 2014; Zhou et al., 2014; Miyazaki et al., 2016; Hackenberg et al., 2017; Mungall et al., 2017; Brüggemann et al., 2018), which may affect the OH reactivity and oxidation capacity (Brüggemann, et al., 2018; Thames et al., 2020). With oceans covering 70% of the Earths' surface, MBL plays an important role in the climate system, affecting particle and cloud formation (Zheng et al., 2021) and the global oxidizing capacity. However, due to the high complexity associated with the logistics of field measurements in the MBL environments, especially if carried out on ships and/or by aircraft (e.g, Mungall et al., 2017; Thames et al., 2020), only limited MBL data are currently available. As a result, the atmospheric chemistry of the MBL is still poorly understood (e.g., Carpenter et al., 2010; Hosaynali Beygi, 2011; Thames et al., 2020)).

Few studies focused on the oxidation capacity and the radical budget in the MBL. While earlier studies suggested that baseline photochemistry in the marine boundary layer can be accurately calculated using simple approaches based on the oxidation of methane and CO (e.g., Penkett, et al., 1997; Cox, 1999), later studies reported missing sources of O₃ (Andrés Hernández et al., 2001) and HCHO (Burkert et al., 2001) indicating the importance of the oxidation of non-methane hydrocarbons (NMHCs). In addition, recent studies show evidence of missing oxidants (e.g., Hosaynali Beygi, 2011) or OH reactivity species (e.g., Thames et al., 2020). Cox (1999) used a simplified box model involving only CO and CH₄ chemistry to simulate the HO_x (OH+HO₂) chemistry during the summer season at two mid-latitude coastal sites in the northern and southern hemispheres (Mace Head, Ireland, and Cape Grim, Tasmania) and concluded that their simplified approach was adequate for defining oxidizing capacity in the unpolluted marine boundary layer. Yang et al., (2004) studied the HO_x chemistry during spring at a northern Atlantic coastal site (Cape Norman, Newfoundland) using a more explicit approach and determined the relative contributions of proxy radicals from several hydrocarbons to ozone formation and found that the production of peroxyl radical is directly related to OH formation from O₃ photolysis. They also found that the variation of the correlation between peroxy radicals and O₃ was significantly higher during spring and suggested an additional RO₂ source (Yang et al., 2004). Carpenter et al. (2010) investigated the seasonal characteristics of HO_x at the Cape Verde Atmospheric Observatory and found a high photochemical activity at the site as demonstrated by maximum measured spring and summer concentrations of OH and HO₂ of 9x10⁶ molecule cm⁻³ and 6x10⁸ molecule cm⁻³, respectively. They also observed higher OVOCs in spring compared to summer, which highlights their important role in regulating the seasonal cycle of the radical budget. Hosaynali Beygi et al.

(2011) investigated the oxidant photochemistry in the Southern Atlantic boundary layer and 85 showed evidence of missing oxidants. Voughan et al., (2012) investigated seasonal observations of HO_x in the remote tropical MBL at the Cape Verde Atmospheric Observatory and showed that HO_x levels were higher in spring, and summer compared to winter, consistent with seasonal variability in j(O¹D) and water vapor concentration. They also noted that average measured OH 90 and HO₂ in the clean remote MBL were lower than in more polluted environments. Recently, Thames et al. (2020) investigated the OH reactivity in the MBL based on data from the NASA Atmospheric Tomography (ATom) campaign, in which instruments on the NASA DC-8 aircraft were deployed to measure OH reactivity. They concluded, from the difference between measured and calculated OH reactivity, that an average missing OH reactivity of 0.5 s⁻¹ is due to unmeasured 95 volatile organic compounds (VOCs) or oxygenated VOCs (OVOCs) associated with oceanic emissions. Therefore, the body of the literature in the recent years suggests an incomplete understanding of the HO_x chemistry in the marine boundary layer, which warrants further investigation.

The marine boundary layer is especially influenced by halogen chemistry which affect HO_x budget via HO₂ reactions with halogen monoxides (XO, X=Br, I) to form a Hypohalous acids (HOX), which photolyze to form OH. HOX can be also lost via its uptake on aerosol particles, R3 (e.g., Carpenter, 2003; McFiggans et al., 2000).

	$XO+HO_2 \rightarrow HOX + O_2$	R 1
105	$HOX + hv \rightarrow OH + X$	R 2
	$HOX + aerosol \rightarrow$	R 3

XO have been measured extensively over the last few decades with reported mean maximum daytime values of 2.5±1.1 pptv and 1.4±0.8 pptv for BrO and IO, respectively (e.g., Sommariva et al., 2006; Read et al., 2008, and references therein). Mahajan et al., (2010) reported a year continuous measurement of XO and reported mean daytime values of 2.8 and 1.5 pptv of BrO and IO over the tropical Atlantic Ocean (Mahajan et al., 2010). Much higher values were reported in the polar MBL, especially during ozone depletion events (e.g., Saiz-Lopez et al., 2007; Pöhler et al., 2010; Liao et al., 2012). No seasonal variability could be established for XO species (Read et al., 2008).

In this study, we present an explicit analysis of the radical budget in the marine boundary layer of Bermuda, during spring and summer, 2019, and investigate the potential impact of halogen chemistry on HO_x budget in the MBL in Bermuda.

2. Methodology

100

110

115

120 Two measurement campaigns were held in spring (April 17th - May 13th) and summer (August 12th - September 12th), 2019, to explicitly analyze the radical budget and HONO formation in the marine boundary layer in Bermuda.

2.1. Measurement site

Measurements took place at the Tudor Hill Marine Atmospheric Observatory, operated by the Bermuda Institute of Ocean Sciences (BIOS). The measurement site (see Figure 1) is located on the west coast of Bermuda (32.2647°N, 64.8788°W). Sampling occurred in a tower at 23-m above the ground and ~53 m above the sea surface. This facility is one of a few marine atmospheric observatories worldwide and offers the ability to make year-round, complex measurements of the atmosphere over the ocean without the use of a research ship or buoy mooring. While the measurement site experiences air masses from different directions, only

air masses of MBL origin (southerly to westerly winds) are investigated in this study. We filter and define the air masses from the open ocean with wind direction >180° as marine air masses. However, even the marine air masses (WD > 180°) were not necessarily pristine. Ship emissions are an important source of pollution in the marine environment and our measurements demonstrate this fact via few spikes in air pollutants during the day, higher in frequency and magnitude in spring compared to summer. We didn't filter these ship emissions' spikes as we consider it part of the marine environment and that eliminating these spikes may lead to a bias in our data evaluation since some data were collected over few hours' time intervals such as VOC and particulate nitrates, which we can't filter for these spikes.

140

135



Figure 1: The Tudor Hill Marine Atmospheric Observatory site in Bermuda, indicated by the red star. The geological location of Bermuda in North Alantic Ocean is indicated by the square on the map. Adopted from google maps.

2.2. Trace Gas Measurements

145

150

Trace gas measurements included, nitrous acid (HONO), nitric acid (HNO₃), nitrogen oxide (NO), nitrogen dioxide (NO₂), ozone (O₃), and particulate nitrates (pNO₃), particulate matter (PM_{2.5} and PM₁₀) and non-methane hydrocarbons (NMHCs). HONO, NO₂, HNO₃, and pNO₃ were measured by long-path absorption photometry (LPAP, Zhu et al., 2022 and references therein). Complementary meteorological data were obtained from the BIOS station. A brief list of the measurement techniques used in this study is shown in Table 1. In addition, NO_x measurements at the Fort Prospect Air Quality (AQ) monitoring station, located close to the center of Bermuda (32°18.1'N, 64°46.0'W), were also obtained for comparison purposes. More

- details about the measurement techniques for all measured species, including their calibration and uncertainty analysis can be found elsewhere (Zhu et al., 2021). C₃-C₁₀ NMHCs were sampled at the Tudor Hill measurement site on adsorption tubes (Air toxics, Markes

 International) using an automated sampling system equipped with a calibrated constant flow pump, applying an airflow of 20 ml/min (Spring) and 40 ml/min (Summer) for 3 hours during
- daytime and 6 hours during nighttime. After sampling, the adsorption tubes were placed in airsealed stainless-steel tubes, stored in a refrigerator, and returned at the end of each measurement campaign to our laboratories at USF for thermal desorption (TD) GC-MS analysis following the US EPA Compendium Method TO-17. The GC-MS system was calibrated using a multipoint dynamic calibration using a standard NIST-certified 1PPM 65-component calibration mixture.
 - dynamic calibration using a standard NIST-certified 1PPM 65-component calibration mixture. All the measurement data were averaged over 10 min time intervals. For VOCs, measured concentrations during each sampling time period (e.g., 3 hours) were used for all 10 minutes time intervals within this the sampling time period (see sec. 3.1).

Table 1: List of measurement techniques used in this study

Parameter	Instrument	D_L
NO	chemiluminescence	32 pptv
NO_2	LPAP	14 pptv
NO_2	chemiluminescence	88 pptv
HONO	LPAP	0.6 pptv
HNO ₃	LPAP	1 pptv
PNO_3	LPAP	8.3 pptv
O_3	UV absorption	1.7 pptv
NMHC's	TD/GC-MS	160 pptv (spring)
		80 pptv (summer)
Solar radiation	Eppley TUV	0.3 W m ⁻²

170 **2.3. Model simulations**

175

180

185

190

195

A zero-dimensional photochemical box model based on the Master Chemical Mechanism, MCMv3.3.1 (Jenkin et al., 2015; http://mcm.leeds.ac.uk/MCM) has been used to evaluate the radical budgets during the spring and summer 2019 campaigns. The MCM photochemical box model system of simultaneous stiff ordinary differential equations (ODEs) was integrated with a variable order Gear's method using the FACSIMILE software (Curtis and Sweetenham, 1987)). The model was constrained by 10 min average diurnal profiles of the following measured parameters: relative humidity, pressure, temperature, NO, NO₂, HONO, HNO₃, O₃, and NMHCSs (see section 3.1). Constant methane levels of 1870 ppbv (NOAA-GMD) were used to constrain the box model simulations. Monthly average CO mixing ratios of ~80 and ~75 ppbv during spring and summer, respectively, were obtained from the MERRA-2 data (MERRA, 2021, see supplemental materials). Since we use only air masses of marine origin, CO values are not expected to change significantly during the day. Since HCHO is not measured, simulated HCHO levels in MCM are based on the photochemical oxidation of constrained measured hydrocarbons. However, since we consider only air masses of MBL origin, emitted HCHO is not expected to contribute significantly to MBL HCHO levels. Photolysis frequencies of O₃, NO₂, HCHO, HONO, HOBr, and HOI were calculated based on measured UV (see Table 1), and the TUV model (Madronich and Flocke, 1998) (see our accompanying paper by Zhu et al., 2022 for more information) and constrained to the model. Other photolysis frequencies are parameterized within the MCM model using a two-stream isotropic scattering model under clear sky conditions (Hayman, 1997; Saunders et al., 2003). The parameterized photolysis rates are calculated as a function of solar zenith angle and adjusted by a scaling factor, calculated from the ratio of UV/TUV and model calculated j(NO₂) values, which considers the effects of varying cloud cover and aerosol scattering. The MCM photochemical model was run for a period of 5 days, constrained with the same measured campaign parameters each day, to generate realistic concentrations for the unmeasured intermediate species. Output from day 5 is used for data evaluation. This model version is henceforth denoted as the base model. A series of rate of production analyses (ROPA) were carried out in order to identify the most important photochemical processes driving the formation and loss of OH and HO₂. Several previous studies employed the MCM to study the HO_x chemistry under high NO_x (e.g., Elshorbany et al., 2009a; 2009b; 2010a) and low NO_x environments (e.g., Elshorbany et al., 2012a), including in the marine boundary layer (e.g., Carslaw et al., 1999a, 1999b, Carpenter et al., 2010) and showed that MCM can reproduce the measured HO_x levels within 20% (e.g., Carpenter et al., 2012). We use a 1σ model error of 25% based on the maximum calculated total uncertainty under typical low-NO_x conditions (Pilling et al., 2008; Kanaya et al., 2011; Feiner et al, 2016).

3. Results and discussions

200

205

210

215

220

225

3.1. Trace gas measurements

Figure 2 shows the 10 min diurnal profile of the measured species used in this study during the spring and summer 2019 campaigns in the MBL in Bermuda. We note that the sampling site was under the influence of local emissions on the island, and thus we filter and define the air masses from the open ocean with wind direction >180° as marine air masses, see sec. 2.1 for more details. We calculate an average day for each of the spring and summer campaigns where simultaneous measurements of marine air masses for all species, including VOCs, are available. During the spring campaign, the days of May 2nd to 4th were characterized by marine air masses (WD > 180°). On May 2nd, only the second half of the day was used (from 1 PM on) since wind speed was very low during the first half of the day (see Figure 2), which data could be impacted by local emissions. During the summer campaign, the days August 25, 26, and 29, were characterized with southern to westerly winds (WD>180°). These days, characterized by marine air masses, were considered for the data analysis of the radical budget in the MBL.

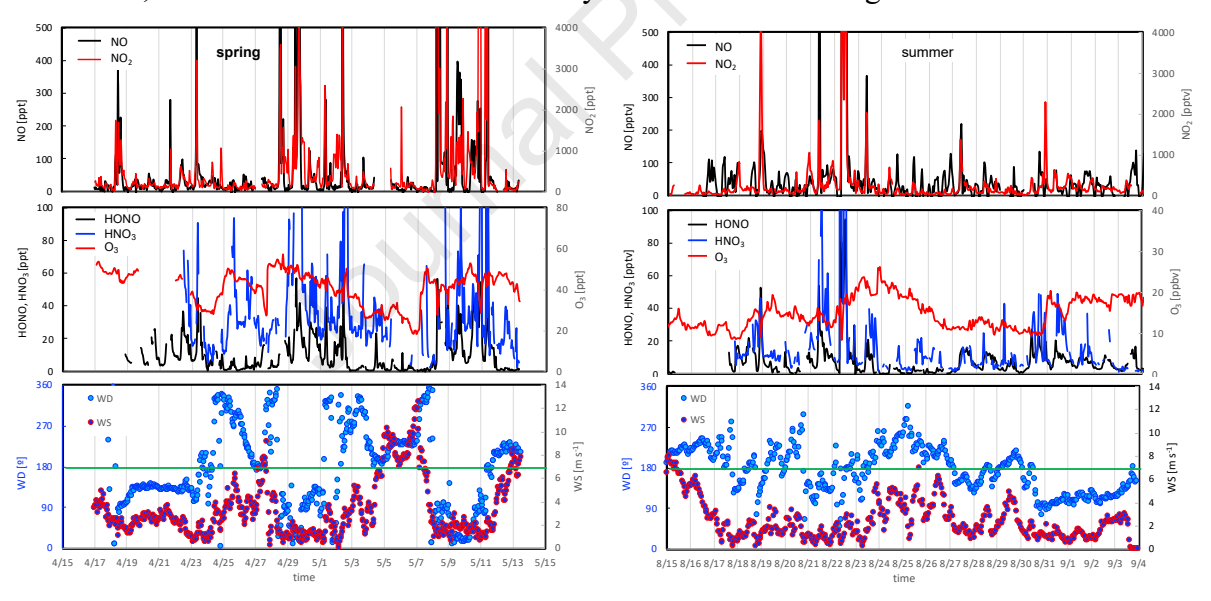


Figure 2: Diurnal profiles of trace gas measurements and wind speed (WS) and wind direction (WD) during the spring and summer campaigns in Bermuda.

Average diurnal profiles of trace gas measurements in the MBL during the spring and summer campaigns in Bermuda are shown in Figure 3 while daytime average values are shown in Table 2. Trace gas concentrations were generally higher in spring compared to summer. Photolysis rate frequencies are comparable during both spring and summer. During spring, air masses were mostly impacted by northwesterly flows that originated from the North American continent. Spring day average O₃, NO_x, HONO, and HNO₃ (see Figure 3) were slightly increased during the afternoon (12:00 to 15:00), which might be due to local ship emissions. During the summer, air masses

originated from circulated air masses above the North Atlantic Ocean (Zhu et al., 2022). Daytime 230 average NO₂ mixing ratios during spring and summer were 170±92 and 84±35 pptv, respectively. NO mixing ratios during spring and summer were ~30±13 and 45±20 ppty, respectively. In comparison, NO₂ and NO average mixing ratios at the Fort Prospect AO monitoring station in the center of the island were 26±5 and 5±4 ppbv (spring, April 17-May 17, 2019), and 6±3 and 10±4 ppbv (summer, August 15-September 4, 2019), respectively, which provide further evidence that there is little to no local influence on the MBL measurements at Tudor Hill. HONO average 235 daytime mixing ratios during the spring and summer were $\sim 3\pm 1$ pptv. These values are much higher than their corresponding nighttime values (Figure 3). Spring ozone levels are about two times that during the summer while $j(O^1D)$ and $j(NO_2)$ values are comparable during spring and summer. Relative humidity (RH) and temperature were higher in summer compared to spring with 240 average daytime levels of 80% and 300 K, respectively during the summer, and 75% and 296 K, respectively, during the spring.

245

250

255

Average total measured mixing ratios of VOCs were ~9000 and 5000 pptC during spring and summer respectively, which corresponds to a diurnal average VOC/NO_x (pptC/pptv) ratio of ~50±25 during both spring and summer (see Figure 3). However, while VOC and NO₂ were higher during spring compared to summer, average NO levels were slightly higher in summer compared to spring (see Figure 3). The VOC/NO_x ratio informs about the relative availability of VOC and NO_x in the air mass but does not necessarily determine if the system is VOC limited or NO_x limited, which can only be inferred from radical budget (Elshorbany et al., 2012a) or ozone sensitivity analyses (e.g., Elshorbany et al., 2009b). During the spring campaign, nighttime VOCs were sampled every 6-8 hours (compared to 3 hours during summer) and therefore average nighttime spring values looks almost stable (see Figure 3). However, since we focus our analysis on daytime HO_x chemistry, the lower variability in nighttime spring VOC levels should not affect our data analysis. Measured total NMHCs concentration shown in Figure 3 does not include several species that were below our method's detection limits (see supplementary), and it does not include oxygenated volatile organic compounds (OVOCs), and therefore these VOC/NOx ratios should be considered as a lower limit. We perform a sensitivity simulation to evaluate the possible impact of a higher NMHCs and OVOC (that may result from the oxidation of NMHCs) levels (see sec. 3.8).

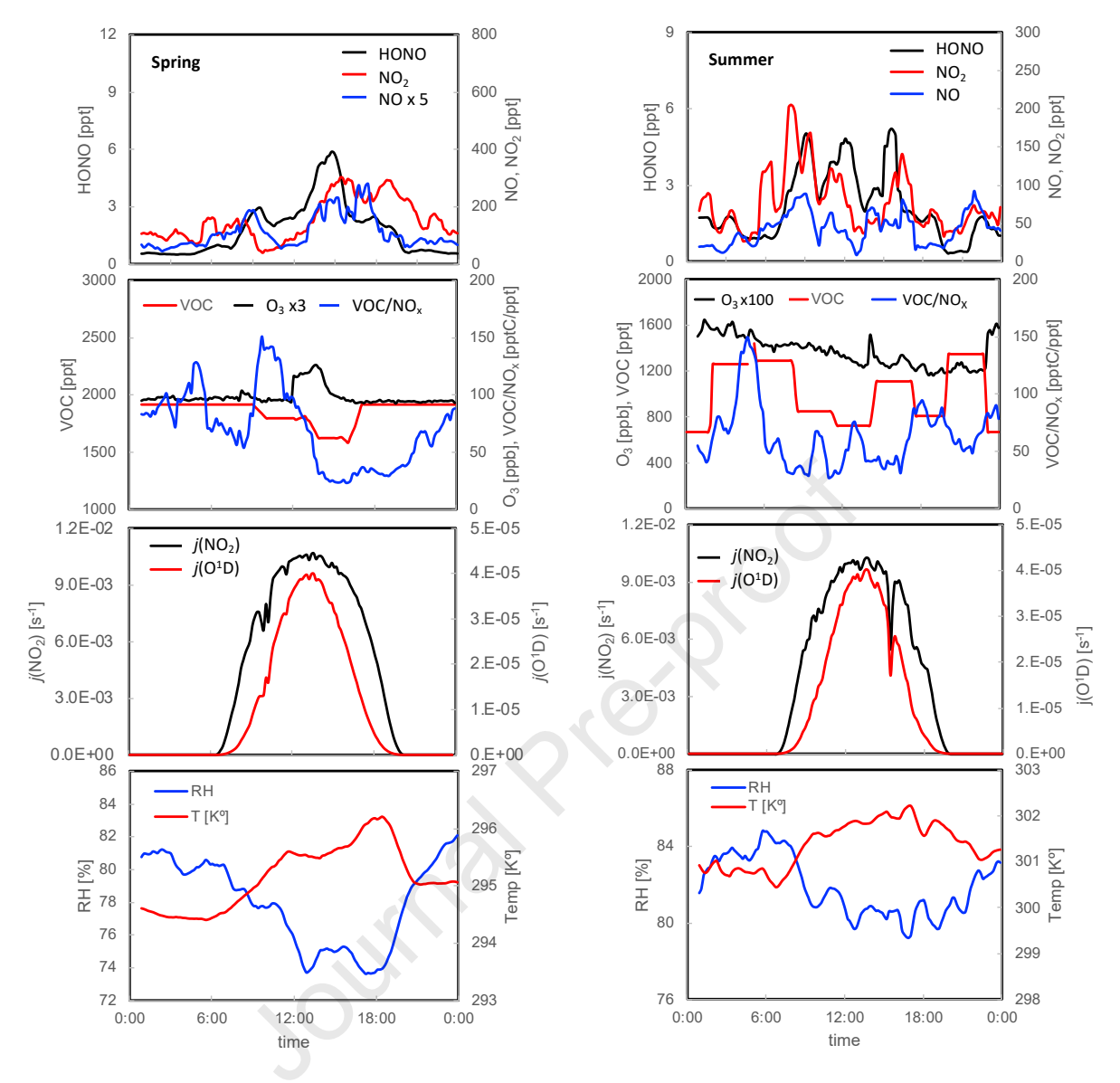


Figure 3: Ten minutes average diurnal profiles MBL (WD > 180°) of simultaneously measured species during the spring and summer 2019 campaigns in Bermuda.

265

270

Measured NMHCs were higher in spring than in summer as shown in Table 2. Average daytime concentrations of the measured NMHCs are quite comparable to those measured in other marine environments (e.g., Greenberg and Zimmerman, 1984; Black et al., 1996; Singh et al., 2000, and references therein). For example, VOC levels in Table 2 are within literature values for propene: 70 to 660 pptv (Greenberg and Zimmerman, 1984; Black et al., 1996), benzene: 40 to 1960 pptv (e.g., Black et al., 1996), and toluene: 30-1490 pptv (Greenberg and Zimmerman, 1984). Ethylbenzene and xylenes originate also from combustion- and petroleum-based emissions and their average daytime mixing ratios are within the range of reported values of 10 to 240 pptv for m- and p-xylenes and 80 to 1100 pptv for ethylbenzene (e.g., Greenberg and Zimmerman, 1984 and references therein). Since only air masses of marine origin are considered, it is unlikely that any of the measured benzene and alkylbenzenes might have resulted from traffic emissions in Bermuda. In addition, since the daytime average lifetime of benzene (1.7-2.2 days), toluene (0.4-

275 0.5 day), and ethylbenzene (0.2-0.4 day) during the study period in spring and summer, respectively, is shorter than the transport time from the continental US (Zhu et al., 2022), they might have originated from marine-based traffic emissions (e.g., ship emissions) as was also concluded in previous studies. Gschwend et al. (1980) and Greenberg and Zimmerman, (1984) showed that measured alkylbenzenes and other hydrocarbons in surface water were sufficient to be in theoretical equilibrium with atmospheric mixing ratios. They attributed the dissolved aromatic hydrocarbons to direct surface water pollution from marine traffic and offshore petroleum production and its subsequent dispersion, which highlights the importance of ship emissions on the marine boundary layer.

Table 2: List of species constrained to the MCM box model and their average daytime values. Refer to Table S1 for a completed list of measured NMHCs.

O I Name	Average Mixing Ratios [pptv]				
Compound Name	Spring	SD	Summer	SD	
O ₃	34063	340	13430	620	
NO	30	13	45	20	
NO ₂	170	92	84	35	
HONO	3.3	1.2	3.2	1.2	
HNO ₃	64	46	12	3	
Propene	485	51	379	23	
Benzene	649	50	296	109	
Toluene	182	14	104	14	
Ethylbenzene	123	10	79	29	
m- & p-xylene	117	9	50	22	

3.2. OH Primary Sources

285

290

295

300

Primary OH sources are responsible for the formation of new OH radicals and include net HONO photolysis, $P_{OH}(HONO) = j[HONO] - k_{OH+NO}[OH][NO]$, ozone photolysis, $P_{OH}(O_3)$, and alkene ozonolysis, $P_{OH}(alkenes)$. Ozone photolysis is the main OH primary source with 0.55 and 0.27 ppb h^{-1} , which accounts for 98% and 97% of the total initiation sources followed by net HONO photolysis, which accounts for 2% and 3%, during the spring and summer, respectively, while alkene ozonolysis accounts for only <1% (Figure 4). The low HONO contribution is due to the very low measured HONO levels of ~3±1 pptv in the MBL in Bermuda, which are lower than that of 11.3 ±1.6 pptv measured over the North Atlantic Ocean near Bermuda (Ye et al., 2016). HONO contribution of up to 80% of OH total initiation sources have been reported in urban high NO_x environments (e.g., Dusanter et al., 2009; Elshorbany et al., 2010a; Zhang et al., 2022) related to the much higher measured HONO levels of several ppbv in these environments. Similarly, the contribution of alkene ozonolysis is negligible in the MBL in Bermuda while significantly higher in polluted environments. These results demonstrate the difference between polluted high NO_x and MBL environments.

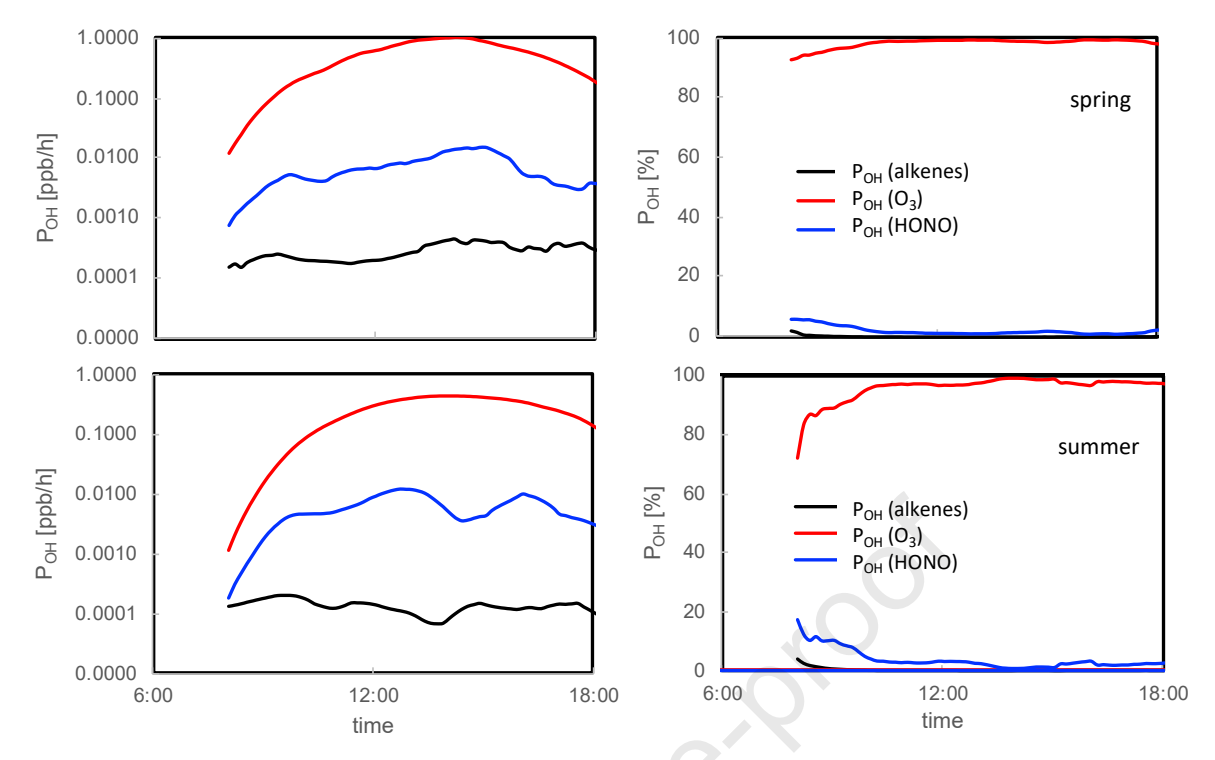


Figure 4: (a) Primary OH production rates from different initiation sources (logarithmic scale) and (b) their relative contribution. $P_{OH}(HONO)$ represents the net HONO photolysis rate defined as $P_{OH}(HONO) = i(HONO) \cdot [HONO] - k_{OH+NO} \cdot [NO] \cdot [OH]$.

3.3. Oxidation Capacity

305

310

315

320

325

The 24 hours average oxidizing capacity (OC) of OH, O₃, and NO₃ is given by their total loss rate due to reactions with VOC and CO, (c.f., Geyer et al., 2001; Elshorbany et al., 2009a) during spring and summer are 3.2x10⁶ and 2.4x10⁶ molecules cm⁻³ s⁻¹ (OH), 7.8x10⁵ and 3.2x10⁵ molecules cm⁻³ s⁻¹ (NO₃), and 1.5 x10⁴ and 2.5x10³ molecules cm⁻³ s⁻¹ (NO₃), respectively. OH is the dominant oxidant accounting for 80% and 87% of the total oxidation capacity followed by O₃ (19% and 12%) during spring and summer, respectively, while nitrate radical accounted for ~1% (see Figure S1). The higher oxidation capacity for all species during spring is due to the higher O₃ (main OH source), VOC, and CO levels compared to summer. The higher relative contribution of O₃ during spring is due to its higher mixing ratios compared to summer. The low contribution of NO₃ radical is due to its fast photolysis during daytime as well as its reaction with NO (see Figure S2). Both spring and summer OC values are about one order of magnitude lower than that reported in urban polluted environments (e.g., Elshorbany et al., 2010a; Mao et al., 2010), which is due to the much lower concentrations of oxidants, NMHCs, and CO in the MBL (see Figure S2).

3.4. Radical budgets

Total production and destruction rates of OH and HO₂ are shown in Figure 5. Total production and destruction ratios of OH (P_{OH}/L_{OH}) and HO₂ (P_{HO2}/L_{HO2}) during spring and summer are around the unity demonstrating the short lifetime and the photo-stationary state of these species. The values of the production and destruction rates of OH and HO₂ are much lower than their corresponding values in more polluted environments which is due to the lower VOC and CO levels in the MBL (see sec. 3.3). During spring, P_{HO2} and L_{HO2} are $\sim 15\%$ lower than P_{OH} and L_{OH} during the morning hours (9 – 13h), which is due to the very low NO levels, under which HO₂ production

from (RO₂+NO→HO₂) and loss (HO₂+NO→OH) is very inefficient. OH and HO₂ production and destruction rates become equal again during the afternoon hours (13 - 18 h) when NO levels almost double. P_{OH}(HO₂+NO) comprised only 14% during the morning hours (9 - 13 h), and 26% during the afternoon hours due to the improved HO₂ production and recycling to OH. In the summer, due to the lower VOC and higher NO levels (compared to spring), the productions and destruction rates of OH and HO₂ are similar.

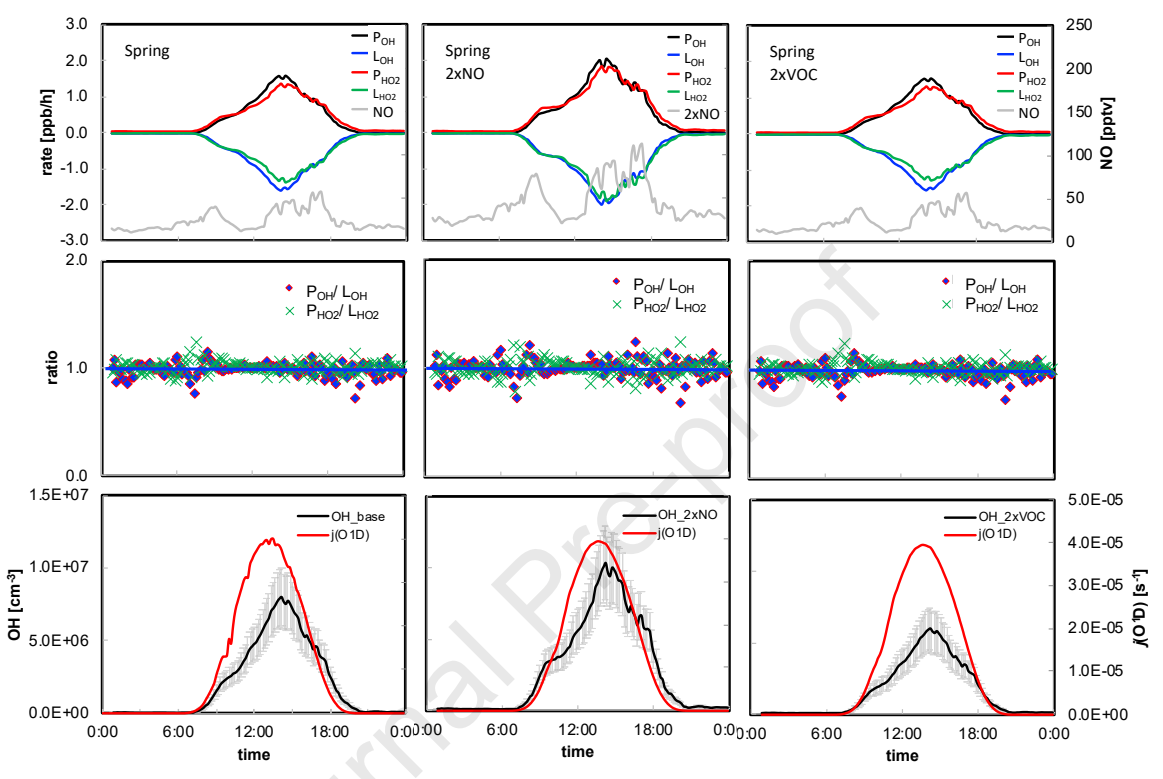


Figure 5: Total production and destruction rates of OH and HO_2 as well as simulated (OH) by the MCMv3.3 for the base scenario, two times NO levels (2xNO) and two times VOC levels (2xVOC) during the spring Bermuda campaign. Error bars on the OH profiles represent 1σ model error.

Simulated daytime (9-18 h) average OH levels are 4.8×10^6 ($\pm 2.0 \times 10^6$) and 4.5×10^6 ($\pm 1.6 \times 10^6$) molecule/cm³ during spring and summer respectively. Spring and summer OH levels reach a maximum of 8.0×10^6 ($\pm 2.0 \times 10^6$) and 7.3×10^6 ($\pm 1.8 \times 10^6$) molecule/cm³, respectively, coinciding with the maximum photolysis frequency of O_3 , $j(O^1D)$. The spring maximum OH is shifted by one hour compared to $j(O^1D)$ due to the O_3 maximum in the afternoon (see Figure 3). These values are comparable to measured OH levels over the North Atlantic Ocean near Bermuda (Ye et al., 2016) and other MBL studies (e.g., Carpenter et al, 2010; Vaughan et al., 2012). The slightly higher OH in the spring is due to the higher O_3 levels compared to summer.

To investigate the system photochemical sensitivity, we vary the levels of NO and VOCs in the model. During the spring, increasing NO levels by two times (2xNO scenario) resulted in higher OH and HO_2 production and destruction rates, with that of HO_2 becoming closer to that of OH (Figure 5). In addition, maximum OH levels have increased by ~50 as a result of the NO increase, which is due to the increase in RO_2/HO_2 recycling to OH. The increase of HO_2 and OH rates as a result of increasing NO demonstrates the NO limited conditions. Increasing VOC levels by two times (2xVOC) has resulted in a decrease in OH levels due to increased loss of OH due to

oxidation of the additional VOCs, forming RO_2 , which are not efficiently recycled back to HO_2 and OH. During the summer, increasing NO levels by two times in the 2xNO scenario enhances maximum OH by ~40% while increasing VOC levels decreases maximum OH by ~20%. These results demonstrate NO limited conditions in spring and summer.

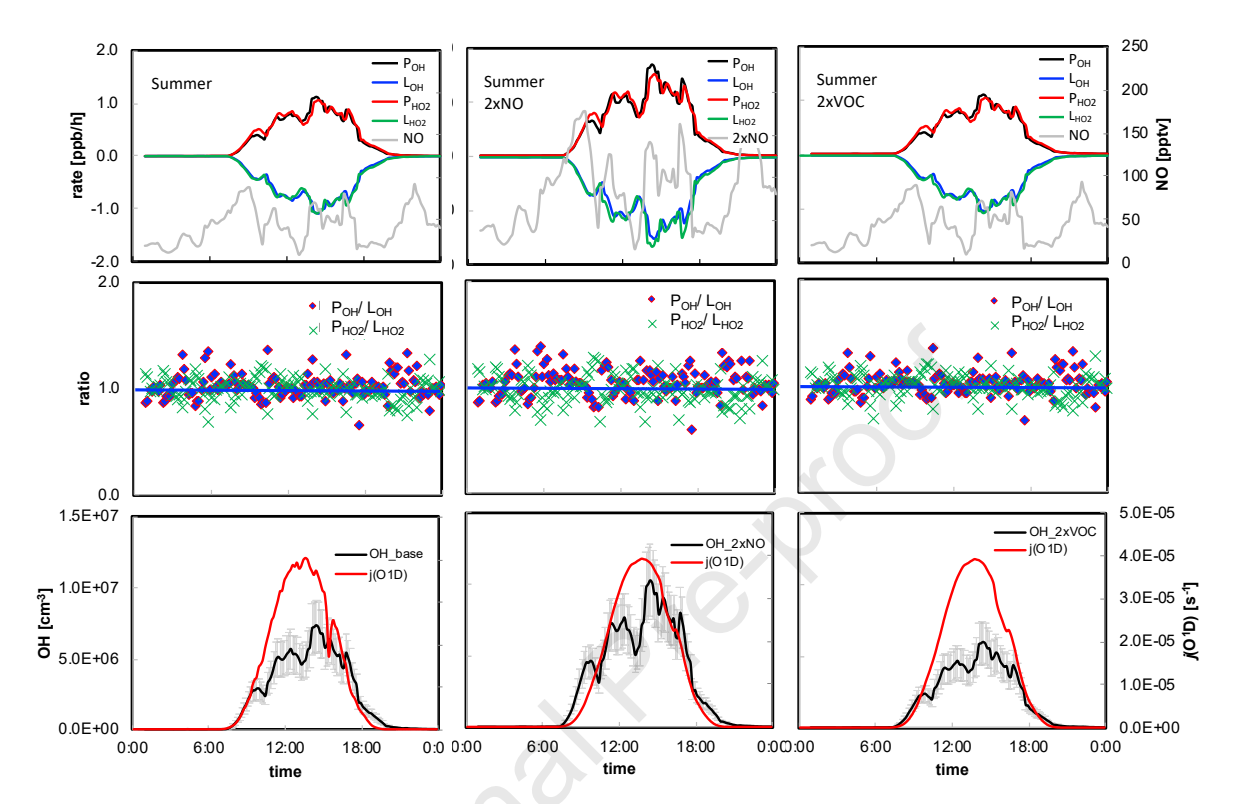


Figure 6: Total production and destruction rates of OH and HO₂ as well as simulated (OH) and calculated OH_{PSS} (P_{OH}/OH reactivity) for the base scenario and using 2xNO during the summer Bermuda campaign. Error bars on the OH profiles represent 1s model error.

3.5. OH Reactivity

360

365

380

The OH reactivity, defined as the reciprocal of the OH radical lifetime, has been calculated as:

OH reactivity
$$[s^{-1}] = L/[OH]$$
 E 1

The calculated mean daytime average OH reactivity is ~1.7±0.06 s⁻¹ and ~1.4±0.02 s⁻¹ during spring and summer, respectively, in Bermuda. These OH reactivities are very low as compared to urban and suburban regions (Elshorbany et al., 2009a, 2012a) but are comparable to previous MBL measurements and modeling studies (e.g., Thames et al., 2020). Thames et al. (2020) found that the measured OH reactivity slightly exceeds calculated OH reactivity in the MBL, which they relate to missing unmeasured VOCs or secondary OVOCs associated with ocean emissions.

Calculated OH reactivity under the 2xVOC scenario shows that an increase in NMHCs increases the OH reactivity by about 30% and 20% during spring and summer, respectively. The increase of the OH reactivity in the 2xVOC scenario is due to the increase in the L_{OH} and the lower simulated OH under this scenario (see sec. 3.4 and E1). Calculated OH reactivity was not significantly affected under the 2xNO scenario since the increase in RO₂ recycling and OH loss is

compensated by the increase in OH (E1) under the prevailing NO limited conditions (see sec. 3.4 and Eq. 1). The increase in the OH reactivity in the 2xVOC scenarios was much higher in the spring due to higher VOC levels. Therefore, the specific impact of VOCs on the OH reactivity depends on the seasonal variability of photochemical regimes. These results suggest that an increase in OVOCs that are formed from NO independent formation pathways, e.g., heterogeneous oxidation on ocean surfaces and ocean emissions (Thames et al., 2020; Wu et al., 2021) would have a larger impact on OH reactivity compared to OVOCs that results from NO-dependent RO₂ recycling, which their formation is reduced by the inefficient recycling of RO₂.

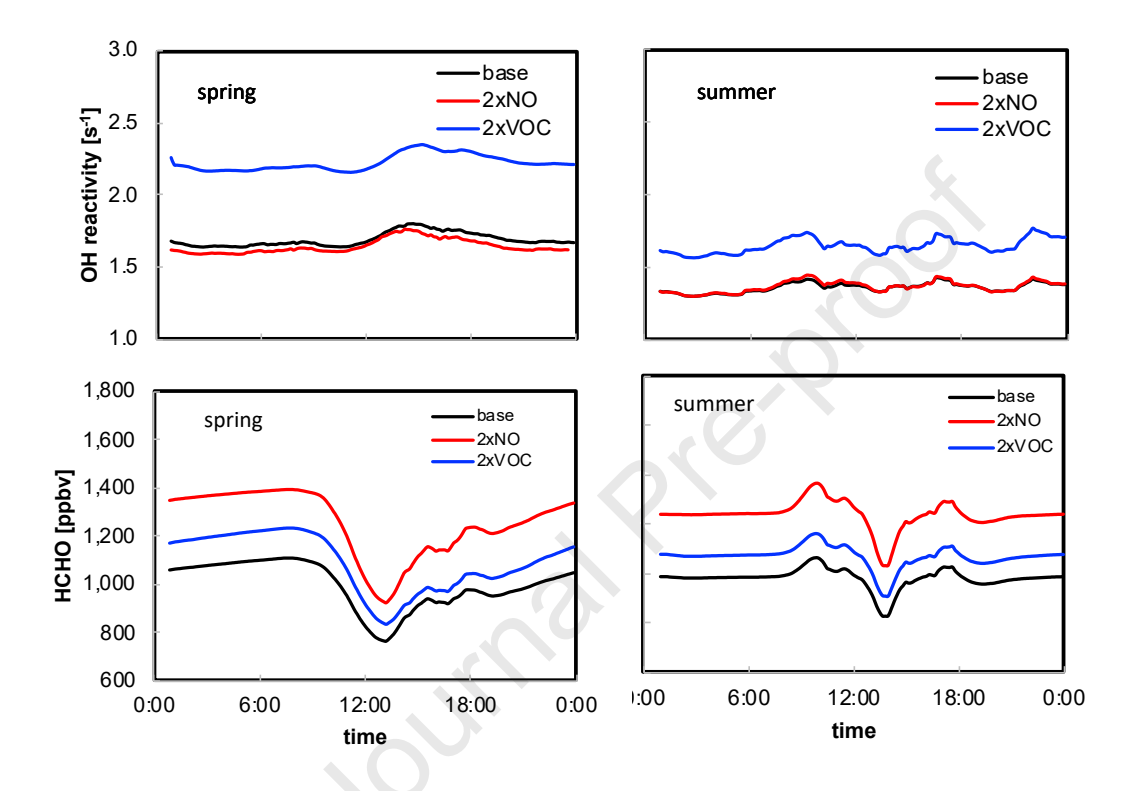


Figure 7: Simulated OH reactivity and HCHO levels during the spring and summer Bermuda campaigns from the base, 2xNO, and 2xVOC scenarios.

To further demonstrate the impact of OVOCs, we investigate the photochemical formation of HCHO under the three scenarios, base, 2xNO, and 2xVOCs. HCHO, mainly a photochemical oxidation product, has background values (mainly based on methane oxidation) of 0.3 - 1 ppbv in the MBL (Jones et al. 2009; Mahajan et al., 2010). Background HCHO levels are relatively stable due to the long lifetime of methane (e.g., Elshorbany et al., 2014) and the low variability of HCHO sinks (Mahajan et al., 2010). Simulated HCHO diurnal profiles show a minimum around the noon hours due to HCHO loss from its photolysis as well as its oxidation with OH, consistent with previous observations of HCHO profiles in the MBL (e.g., Mahajan et al., 2010). Simulated HCHO levels in the Bermuda MBL of 977 pptv (± 61 pptv) during spring and summer, respectively, are comparable to that measured in the tropical Atlantic MBL (Mahajan et al., 2010). Increasing VOC levels (2xVOC scenario) lead to only a small increase of 9% in HCHO levels, due to the inefficient oxidation of RO₂. In addition, the increase in HCHO didn't enhance OH levels (via HCHO +hv \rightarrow HO₂+NO \rightarrow OH) due to the low NO_x conditions. These results further suggest that a missing OH

reactivity in the MBL would be significantly enhanced by an oceanic source rather than a secondary oxidation product, consistent with earlier results (Thomas et al. 2020).

3.6. Radical Propagation

415

420

425

430

435

In this section, we investigate the radical propagation, and secondary radical balance during the spring and summer campaigns. Oxidation of hydrocarbons with OH results in the formation of alkyl peroxy radicals (RO₂). Efficient recycling of RO₂ to HO₂ and HO₂ to OH requires a sufficient amount of NO. In addition, OH oxidation of CO and hydrocarbons results in the direct formation of HO₂ (P_{HO2}(OH→HO₂). Average daytime simulated RO₂/HO₂ ratios of 1.6 (±0.29) in the spring and 1 (±0.25) in the summer (Figure 8) indicate a higher oxidation rate in the summer (OH+RH→RO₂), which is due to the higher NO and lower VOC levels in the latter (Figure 8). In addition, the maximum total peroxy radical (RO₂+HO₂) concentrations of 75 and 62 pptv during spring and summer, respectively (see Figure 8)) are very high in comparison to high NO_x environments (Mihelcic et al., 2003; Hofzumahaus et al., 2009; Elshorbany et al., 2009a) but similar to that of low NO condition (e.g, Elshorbany et al., 2012a), and in agreement with previously reported RO₂+HO₂ measurements over the North Atlantic Ocean off North Carolina coast (Ye et al., 2016) as well as in other remote marine environments (e.g., Kanaya et al., 2001; Lee et al., 2010; Carpenter et al., 2010; Vaughan et al., 2012, and references therein).

The HO₂/OH ratio is a measure of the recycling efficiency related to HO₂ reaction with NO which regenerates OH (e.g. Fleming et al., 2006; Emmerson et al., 2007; Dusanter et al., 2009; Elshorbany et al., 2010a). Daytime average HO₂/OH of 85(±22) and 100(±41) during spring and summer, respectively, are high and are typical of low NO₂ marine environments (Kanaya et al., 2001; Fleming et al., 2006; Carpenter et al., 2010; Vaughan et al., 2012, and references therein) compared to high NO₂ urban conditions (e.g., Elshorbany et al., 2009a, and b; Zhang et al., 2022). Simulated diurnal HO₂/OH profiles during spring show a fast-declining ratio from ~120 at 9:00 to ~50 at 15:00, coinciding with increased RO₂/HO₂ ratio due to increased OH oxidation under limited NO levels. HO₂/OH ratios show the expected inverse correlation with NO (Figure 8) since HO₂ reaction with NO is the main HO₂ sink (e.g., Fleming et al., 2006). However, the correlation is less robust compared to high NO₂ environments (e.g., Elshorbany et al., 2009a, and b; Zhang et al., 2022), which is due to the much lower contribution of HO₂ recycling (HO₂+NO→OH) to OH (see secs. 3.4 and 3.7). These results are consistent with HO₂ observations in other marine environments (e.g., Vaughan et al., 2012).

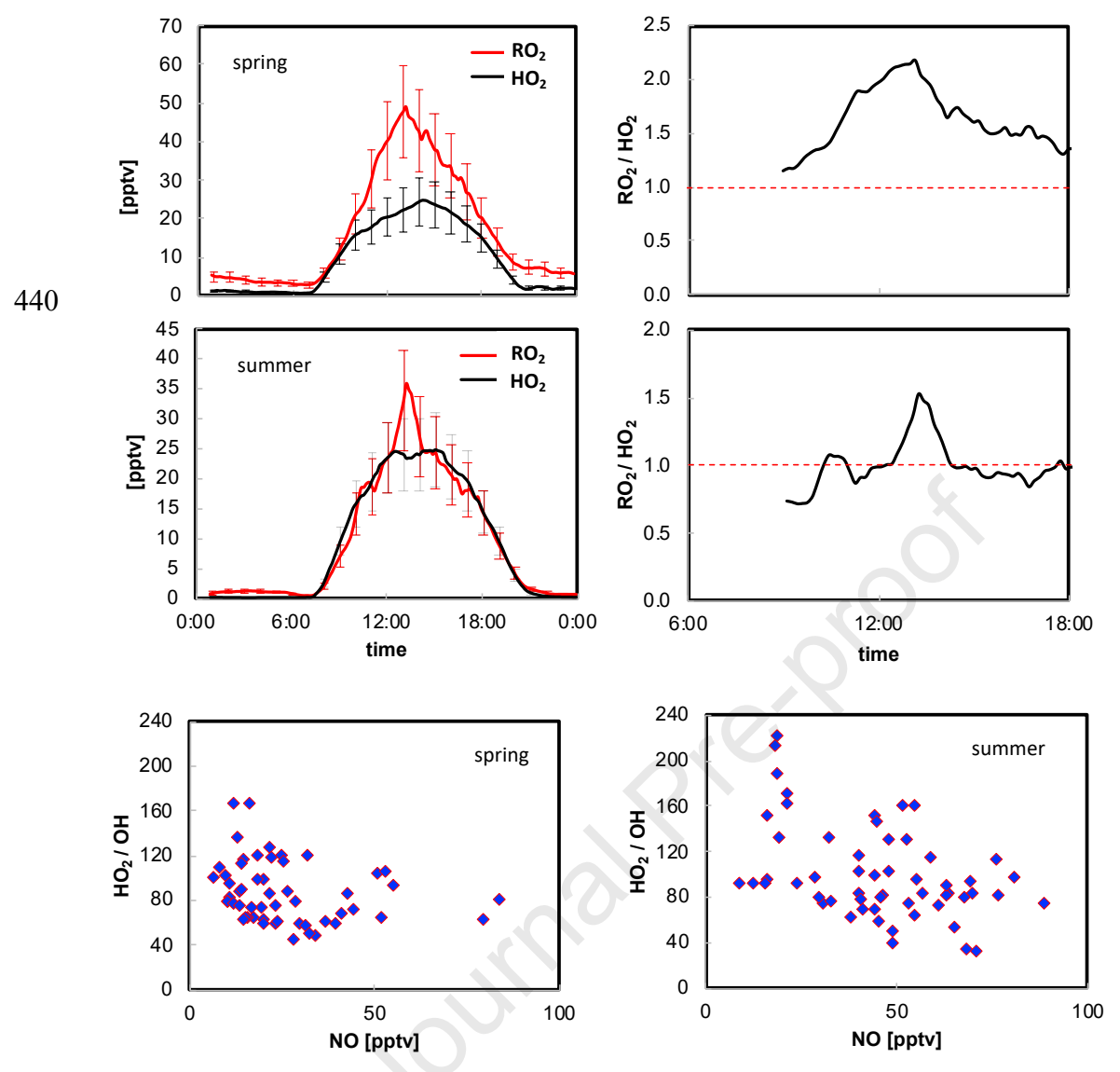


Figure 8: Diurnal profiles of simulated RO₂ and HO₂, RO₂/HO₂, and the correlation between HO₂/OH and NO for the Bermuda spring and summer measurement campaigns. Error bars represent 1σ model error and are shown every hour for clarity.

3.7. Radical Fluxes

445

455

Average daytime fluxes of key OH radical sources and sinks during the spring and summer Bermuda campaign calculated by the MCMv3.3 are shown in Figure 9. We define below some parameters to further explore the radical budget analysis.

450 O Total production of OH, P_{OH} = P_R + P_{OH}(sec), where:

$$P_R = j(HONO)[HONO] + j(O^1D)[O_3]\Phi_{OH} + \Sigma k_{O_3+alkene}[alkene][O_3]\Phi_{OH}$$

$$P_{OH}(sec) = P_{OH}(HO_2 \rightarrow OH) + P_{OH}(others)$$

where P_{OH}(HO₂→OH): production of OH by HO₂+NO and HO₂+O₃ reaction, P_{OH}(others): production of OH from other minor secondary sources (photolysis of H₂O₂, ROOH, and RO decomposition as well as RCO₃ reaction with HO₂.

- O Total loss of OH, $L_{OH} = L_R + L_{OH}(sec)$, where $L_R = k_{NO_2+OH}[NO_2][OH] + k_{OH+NO}[NO][OH]$ $L_{OH}(sec)$, loss of OH due to oxidation of CO and hydrocarbons: $L_{OH}(sec) \approx L_{OH} - [L_{OH}(NO) + L_{OH}(NO_2)]$, or alternatively $L_{OH}(sec) \approx L_{OH}(OH \rightarrow HO_2) + L_{OH}(OH \rightarrow RO_2)$
- o Total production of HO₂, P_{HO2}=P_{HO2}(OH→HO₂)+P_{HO2}(sec), where P_{HO2}(OH→HO₂) is HO₂ production rate from OH reactions with HCHO, CO, H₂, O₃, and VOCs. P_{HO2}(sec) is HO₂ production rate from other sources, e.g., photolysis of OVOCs, and alkene ozonolysis.
- O Total loss of HO₂, L_{HO2}=L_{HO2}(NO)+L_{HO2}(O₃)+L_{HO2}(sec), where L_{HO2}(NO) and L_{HO2}(O₃) are the HO₂ loss rates due to its reaction with NO and O₃, respectively. L_{HO2}(sec) is the HO₂ loss rate due to its self- and cross-reactions with HO₂ and RO₂ as well as its reaction with OH and NO₂.

The oxidation of hydrocarbons with OH leads to the formation of RO₂ and HO₂. During the spring, RO₂ production rate is much higher during spring compared to summer due to the higher VOC levels in the spring. However, due to the lower NO levels in the spring, RO₂ radicals are not efficiently recycled to HO₂ resulting in the high RO₂/HO₂ and HO₂/OH ratios (see Figure 8). In the summer, RO₂/HO₂ ratios are smaller due to the lower VOC levels but HO₂/OH ratio is still relatively high due to the prevailing NO limited conditions.

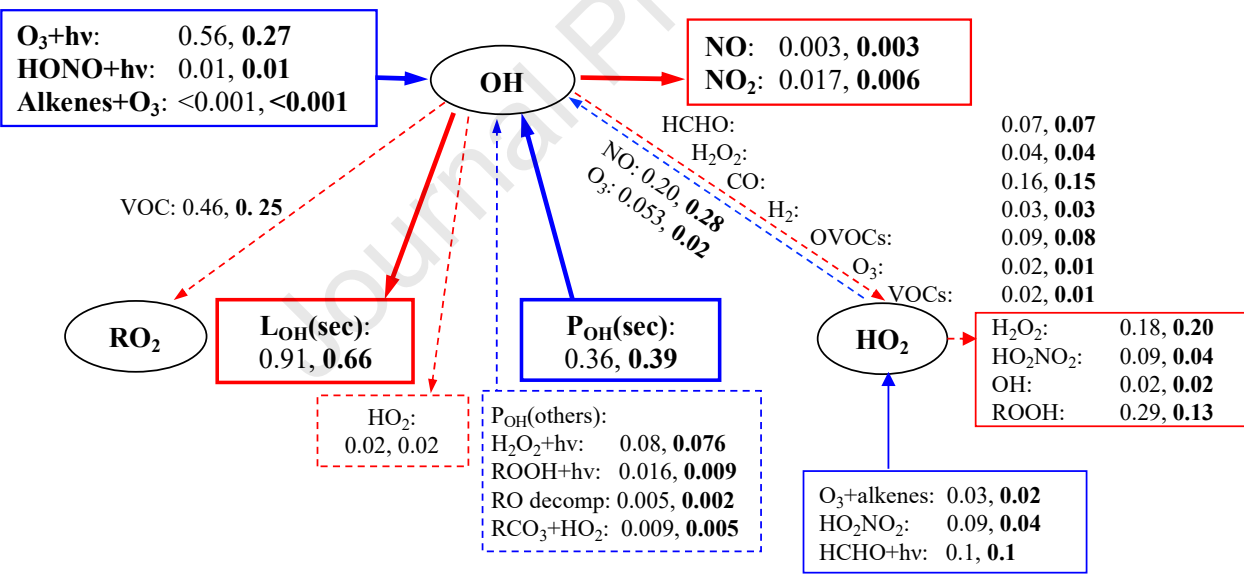


Figure 9: Average fluxes (09:00–18:00) of the key radical sources and sinks during the Bermuda spring and summer (bold) campaigns calculated by the MCMv3.3. Units are in ppb h⁻¹. The box with blue dashed lines contains minor secondary OH sources, P_{OH}(others), together with P_{OH}(HO₂+NO) and P_{OH}(HO₂+O₃) (dashed blue arrows), they make the P_{OH}(sec). The box with red dashed lines is a minor OH secondary loss, together with L_{OH}(OH→HO₂)+L_{OH}(OH→RO₂) (dashed red arrows) they make the secondary OH loss, L_{OH}(sec).

475

480

485

OH initiation sources (P_R) made 61% and 42% of the total OH production rate during the daytime (9 - 18 h) in spring and summer, respectively. OH oxidation of hydrocarbons forming RO₂ (($L_{OH}(OH \rightarrow RO_2)$, 49%, 37%) and HO₂ (($L_{OH}(OH \rightarrow HO_2)$, 46%, 60%) are the main OH

loss rates followed by its reaction with NO_x (2%, 1%), during spring and summer, respectively. Thus, the secondary loss of OH, L_{OH}(sec) represents the vast majority of OH loss of ~98% during spring and summer. Recycling these oxidized radical species to OH requires a sufficient amount of NO. However, the HO₂ reaction with NO (P_{OH}(HO₂+NO), accounts for only 22% and 42% of the total OH production (P_{OH}) during spring and summer, respectively. These rates are much lower than those reported for urban (Elshorbany et al., 2009a; Zhang et al., 2022) and suburban (Elshorbany et al., 2012a; Kanaya et al., 2012) conditions in which P_{OH}(HO₂+NO) accounts for up to 80% of the total OH radical budget. The lower P_{OH}(HO₂+NO) fraction during the spring is due to the very low NO levels. HO₂ reaction with O₃ is an important source of OH in low-NO_x environments, contributing about 6% during spring compared to only 3% in summer, due to the higher O₃ levels in the earlier. Another important secondary OH production term, include H₂O₂ photolysis, which accounts for 9% and 11% during spring and summer, respectively.

During spring and summer, HO₂ main source is the OH reaction with CO, HCHO, H₂, O₃, and VOCs (P_{HO2}(OH→HO₂), 52%, 58%) followed by HCHO photolysis, 12%, 14%, HO₂NO₂ thermal decomposition, 11%, 6% (reversible reaction), and alkene ozonolysis (4% and 3%)) and the rest come from RO decomposition and reactions with O2. HO2 destruction due to its reaction with NO, L_{HO2}(NO), account for only 24% and 41% while HO₂ self-reaction to form H₂O₂ and cross-reaction with RO₂ to form ROOH, together make about 56% and 48% during spring and summer, respectively. The HO₂ loss due to reaction with O₃ (L_{HO2}(O₃) is 6% in spring compared to 3% in summer. We note that HO₂ loss due to NO is higher in summer compared to spring while HO₂ loss due to self-and cross-reactions with other radicals is higher in spring compared to summer, which demonstrates the more NO limited regime leading to inefficient recycling in spring compared to summer. The higher HO₂ production from HO₂ self and cross-reactions in both seasons demonstrate the NO limited regime in the tropical North Atlantic Ocean. Furthermore, the balance ratio, (BR = $P_{OH}(sec)/L_{OH}(sec)$, Elshorbany, et al., 2010a), which is a measure of the secondary recycling of OH radical has a value of 0.4 during spring indicating limited NO conditions increasing to 0.6 during summer indicating a better recycling but is still not efficient enough to reach efficient recycling at a BR ratio of 1 (Elshorbany et al., 2010a). These results above shed light on the NO-limited conditions in the tropical north Atlantic MBL and their recycling mechanism towards a better understanding of the HO_x chemistry in this important but remote environment.

3.8. Impacts of Halogen on HOx budget.

500

505

510

515

520

525

530

Halogen chemistry can affect the HO_x budget, potentially decreasing HO₂ and increasing OH, via reactions R1 to R3 (e.g., Sommariva et al., 2006; Read et al., 2008; Mahajan et al., 2010; Whalley et al., 2010; Liao et al, 2012). The reduction of HO₂ and formation of HOX depend on the abundance of XO and HO₂. Measured XO mean daytime values in the tropical Atlantic Ocean are within 2.5 ± 1.1 pptv and 1.4 ± 0.8 pptv for BrO and IO, respectively (e.g., Sommariva et al., 2006; Read et al., 2008, and references therein) with no established seasonality. HOX can be also lost via its uptake on aerosol particles (e.g., Carpenter, 2003; McFiggans et al., 2000). Since BrO and IO levels were not measured in Bermuda, we use the mean values of 2.5 pptv and 1.4 pptv (Read et al., 2008), respectively, as constant mixing ratios in our sensitivity analysis to investigate their possible impacts on HO_x. HOX loss to aerosol particles depends on their uptake coefficient in addition to the aerosol surface area. We calculate aerosol uptake in our model based on the following free molecular expression: $K_{het} = \frac{A\gamma v}{4}$, where K_{het} is the heterogeneous rate constant (s⁻¹), A is the aerosol surface area, γ is the uptake coefficient, ν is HOX mean molecular speed. A =

 $4\Pi r^2N$, where r is the average radius of aerosol particles and N is aerosol number concentration, the number of particles per unit volume. We used representative values for r=150 nm and N = 1000 cm⁻³ in Bermuda based on global model simulations and measurements of aerosol properties (Spracklen et al., 2010; Lee et al., 2010; Elshorbany et al., 2014; Ranjithkumar et al., 2021; Dadashazar et al., 2021). This results in an A value of 2.83x10⁻⁶ cm² cm⁻³, which is within the literature values of 1 x10⁻⁶ cm² cm⁻³ (Mahajan et al., 2010) and 0.51x10⁻⁶ cm² cm⁻³ (Liao et al., 2012), and 1 x10⁻⁷ cm² cm⁻³ (Read et al., 2008). The molecular speed, υ , is calculated as 8RT/πM, where R is the general gas constant, T, temperature, and M is the HOX molecular weight. Calculated average HOX molecular speeds are 257 and 210 m s⁻¹ for HOBr and HOI, respectively. Steady State concentrations of HOX, [HOX]_{ss}, can be calculated using the following equation (Liao et al., 2012):

 $P_{HOX} = L_{HOX}$

535

540

545

550

555

560

565

 $P_{HOX} = k_{XO+HO2}[XO][HO_2]$

 $L_{HOX} = j(HOX)[HOX] + k_{het}[HOX)$, where k_{het} is the heterogeneous rate constant of HOX on aerosol particles, j(HOX) is the photolysis rate of HOX.

[HOX]ss =
$$\frac{k_{XO+HO2}[XO][HO2]}{j(HOX)+k_{het}}$$
 E 1

During spring and summer, including halogen chemistry decreased HO₂ by $14\sim\%$ and $\sim18~\%$, respectively while OH changed by only 3% and -1%, respectively, see supplementary materials and Figure 10. The reduction of HO₂ leads to a corresponding reduction in HO₂ recycling (see sec. 3.7). Therefore, the low impact of HOX photolysis on OH is due to the competition of R1 and R2 with PoH(sec), and the loss of HOX by aerosol uptake. In addition, the increase in OH from HOX photolysis in spring is due to the lower contribution of PoH(sec) to PoH compared to summer. During the summer, the production of OH from the photolysis of HOX was not sufficient to compensate the HO₂ loss due to reaction with OX. Therefore, the photolysis of HOX was more important during spring due to the lower NO conditions as the reaction of HO₂+NO becomes less important and the loss of HO₂ via reaction with XO becomes an alternative recycling pathway to OH.

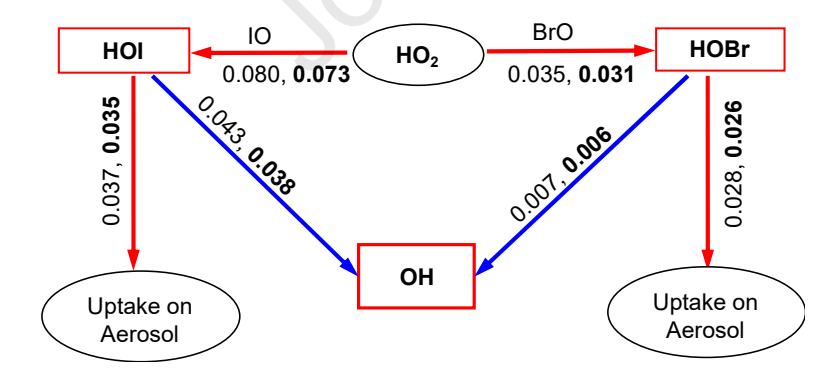


Figure 10: Average fluxes (09:00–18:00) of HOBr and HOI sources and sinks during the Bermuda spring and summer (bold) campaigns calculated by the MCMv3.3. Units are in ppb h⁻¹.

The daytime average loss of HO₂ due to reaction with IO (L_{HO2}(IO)) is 0.080 and 0.073 ppb/h compared to only 0.035 and 0.031 ppb/h for BrO (L_{HO2}(BrO)), during spring and summer, respectively, which is due to the higher reaction rate of for IO, k_{HO2+IO} (1.4×10⁻¹¹ $e^{540/T}$), compared

to that of BrO of $3.4 \times 10^{-12} e^{540/T}$ (e.g., Liao et al., 2012). HOBr is mainly lost via aerosol uptake, which accounts for ~80% of the HOBr loss term while photolysis accounts for only ~20%. However, HOI photolysis accounts for almost 50% of its total loss rate, due to its much higher photolysis rate compared to HOBr. Therefore, OH production from HOI is ~6 times higher than that of HOBr. The competition between aerosol uptake and photolysis as the two main loss processes for HOX highlights the importance of aerosol uptake on OH production from HOX photolysis, i.e., higher aerosol uptake leads to lower OH production via HOX photolysis. These results are consistent with earlier reports (e.g, Sommariva et al., 2006; Read et al., 2008; Lee et al., 2010; Liao et al., 2012) and further demonstrate the need for more comprehensive HO_x, VOC, halogens, and aerosol measurements in the MBL towards a better understanding of global atmospheric chemistry and climate.

4. Conclusion

580 In this study, we analyzed data from two field measurement campaigns during the spring and summer of 2019 in the marine boundary layer of Bermuda. We simulated the radical budget of OH, HO₂, and RO₂ using a box model based on the MCMv3.3.1. Measured concentrations of all species except NO were higher in the spring than during the summer. The higher ozone and VOC levels in the spring lead to a higher OH oxidation rate of CO and hydrocarbons compared to 585 summer. The radical budget analysis demonstrates a NO_x-limited regime, leading to inefficient recycling of RO₂ and HO₂ to OH, more apparent in spring compared to summer. The imbalance between secondary OH production (PoH(sec)) and loss (LoH(sec)) is higher in spring compared to summer. Simulated OH reactivities of $\sim 1.7 \pm 0.06 \text{ s}^{-1}$ and $\sim 1.4 \pm 0.02 \text{ s}^{-1}$ during spring and summer. respectively, are very low compared to urban and suburban regions but agree with recent 590 measurements in the marine boundary layer. OH reactivity, and radical budget analysis infers inefficient recycling and suggests that missing OH reactivity sources of marine origin rather than OH secondary oxidation products, which their formation is diminished by the NO limited conditions. We also investigated the role of halogen monoxides, XO on HO_x using mean measured XO values in the Atlantic Ocean. Halogen monoxides, BrO and IO, were found to decrease HO₂ 595 by ~14 and 18% during spring and summer, respectively, with only marginal impact on OH as HOBr and HOI loss to aerosol particles accounts for ~80 and ~50% of their total loss term, respectively. The results demonstrate the complex multiphase HO_x-Halogen-aerosol chemistry in the MBL and call for more comprehensive multiphase investigations. Our results suggest the need for comprehensive multiphase gradient measurements of halogens, VOC, and OVOCs, i.e., at the 600 air-sea interface, and at higher altitudes to better understand the radical budget in the MBL and its impact on global climate.

5. Acknowledgments

We acknowledge funding from the NSF AGS-1826956 (Yasin Elshorbany), AGS-1900795 (Yasin Elshorbany), AGS-1826989 (Xianliang Zhou), OCE-1829686 (Andrew Peters), and from Chinese National Science Foundation Awards #41875151 (Chunxiang Ye).

6. References

605

Anderson, J. R., Buseck, P. R., Patterson, T. L., and Arimoto, R.: Characterization of the Bermuda tropospheric aerosol by combined individual-particle and bulk-aerosol analysis, Atmos. Environ., 30, 319–338, https://doi.org/10.1016/1352-2310(95)00170-4, 1996.

- Andrés-Hernández, M., J. Burkert, L. Reichert, D. Sto"bener, J. Meyer- Arnek, J. P. Burrows, R. R. Dickerson, and B. G. Doddridge (2001), Marine boundary layer peroxy radical chemistry during the AEROSOL99 campaign: Measurements and analysis, J. Geophys. Res., 106, 20,833–20,846, 2001.
- Arnold, S.R., Spracklen, D.V., Gebhardt, S., Custer, T., Williams, J., Peeken, I., Alvain, S.:

 Relationships between atmospheric organic compounds and air-mass exposure to marine biology. Environ. Chem. **7**(3), 232–241, 2010.
 - Baker, A. R. et al. Distribution and sea-air fluxes of biogenic trace gases in the eastern Atlantic Ocean. Glob. Biogeochem. Cycles 14, 871–886, 2000.
- Bates, T. S., Patricia K. Quinn, David S. Covert, Derek J. Coffman, James E. Johnson & Alfred Wiedensohler: Aerosol physical properties and processes in the lower marine boundary layer: a comparison of shipboard sub-micron data from ACE-1 and ACE-2, Tellus B: Chemical and Physical Meteorology, 52:2, 258-272, DOI: 10.3402/tellusb.v52i2.16104, 2000.
- Brüggemann, M., Hayeck, N., George, C.: Interfacial photochemistry at the ocean surface is a global source of organic vapors and aerosols, Nature Communications, 9, 1, https://doi.org/10.1038/s41467-018-04528-7, 2018.

- Burger, J. M., Granger, J., Joyce, E., Hastings, M. G., Spence, K. A. M., and Altieri, K. E.: The importance of alkyl nitrates and sea ice emissions to atmospheric NO_x sources and cycling in the summertime Southern Ocean marine boundary layer, Atmos. Chem. Phys., 22, 1081–1096, https://doi.org/10.5194/acp-22-1081-2022, 2022.
- Burkert, J., M. Andre's-Herna'ndez, D. Sto"bener, J. P. Burrows, M. Weissenmayer, and A. Kraus, Peroxy radical and related trace gas measurements in the boundary layer above the Atlantic Ocean, J. Geophys. Res., 106, 5457–5477, 2001.
- Cantrell, C. A., R. E. Shetter, T. M. Gilpin, J. G. Calvert, F. L. Eisele, and D. J. Tanner: Peroxy radical concentrations measured and calculated from trace gas measurements in the Mauna Loa Observatory Photochemistry Experiment 2, J. Geophys. Res., 101, 14,653–14,664, 1996.
 - Cantrell, C. A., et al., Steady state free radical budgets and ozone photochemistry during TOPSE, J. Geophys. Res., 108(D4), 8361, doi:10.1029/2002JD002198, 2003.
- 640 Carpenter, L. J., P. S. Monks, B. J. Bandy, S. A. Penkett, I. E. Galbally, and C. P. Meyer, A study of peroxy radicals and ozone photochemistry at coastal sites in the Northern and Southern Hemispheres, J. Geophys. Res., 102, 25,417–25,427, 1997.
 - Carpenter, L.J., Lewis, A.C., Hopkins, J.R., Read, K.A., Gallagher, M., Longley, I.: Uptake of methanol to the North Atlantic ocean surface. *Global Biogeochem. Cycles.* **18**, 2004.

- 645 Carpenter, L.J., Fleming, Z.L., Read, K.A. *et al.* Seasonal characteristics of tropical marine boundary layer air measured at the Cape Verde Atmospheric Observatory. *J Atmos Chem* **67**, 87–140 (2010). https://doi.org/10.1007/s10874-011-9206-1, 2010.
- Carslaw, N., D. J. Creasey, D. E. Heard, A. C. Lewis, J. B. McQuaid, M. J. Pilling, P. S. Monks, B. J. Bandy, and S. A. Penkett, Modeling OH, HO₂, and RO₂ radicals in the marine boundary layer: 1. Model construction and comparison with field measurements, J. Geophys. Res., 104, 30,241–30,255, 1999a.
 - Carslaw, N., P.J. Jacobs, M. J. Pilling: Modeling OH, HO, and radicals in the marine boundary layer, 2. Mechanism reduction and uncertainty analysis, J. Geophys. Res., 104, D23, 30,257-30,273, 1999b.
- 655 Cox, R. A.: Ozone and peroxy radical budgets in the marine boundary layer: Modeling the effect of NO_x, J. Geophys. Research, https://doi.org/10.1029/1998JD100104, 1999
 - Dadashazar, H., Alipanah, M., Hilario, M. R. A., Crosbie, E., Kirschler, S., Liu, H., Moore, R. H., Peters, A. J., Scarino, A. J., Shook, M., Thornhill, K. L., Voigt, C., Wang, H., Winstead, E., Zhang, B., Ziemba, L., and Sorooshian, A.: Aerosol responses to precipitation along North American air trajectories arriving at Bermuda, Atmos. Chem. Phys., 21, 16121–16141, https://doi.org/10.5194/acp-21-16121-2021, 2021.

660

- Elshorbany, Y. F., Kurtenbach, R., Wiesen, P. Lissi, E., Rubio, M., Villena, G., Gramsch, E., Rickard, A. R., Pilling, M. J., Kleffmann. J.: Oxidation capacity of the city air of Santiago, Chile, *Atmospheric Chemistry and Physics*, 9, 2257-2273, 2009a.
- 665 Elshorbany, Y. F, Kleffmann, J., Kurtenbach, R., Rubio, R., Lissi, E., Villena, G., Rickard, A.R. and Pilling, M. J., Wiesen, P.: Summertime Photochemical Ozone Formation in Santiago de Chile, *Atmospheric Environment*, 43, 6398-6420, 2009b.
 - Elshorbany, Y. F, Kleffmann, J., Kurtenbach, R., Rubio, R., Lissi, E., Villena, G., Rickard, A.R. and Pilling, M. J., Wiesen, P.: Seasonal dependence of the oxidation capacity of the city of Santiago de Chile, *Atmospheric Environment*, 44, 5383-5394, a special issue dedicated for the Atmospheric Chemical Mechanism conference, ACM-2009, Davis, US, 2010a.
 - Elshorbany, Y. F, Barnes, I., Becker, K. H, Kleffmann, J., and Wiesen, P.: Sources and Cycling of Tropospheric Hydroxyl Radicals-An Overview, *Zeitschrift für Physikalische Chemie*, 224, 967-987, DOI:10.1524/zpch.2010.6136, 2010b.
- Elshorbany, Y. F., Kleffmann, J., Hofzumahaus, A., Kurtenbach, R., Wiesen, P., Dorn,H.-P.,
 Schlosser, E., Brauers, T., Fuchs, H., Rohrer, F., Wahner, A., Kanaya, Y., Yoshino, A.,
 Nishida, S., Kajii, Y., Martinez, M., Rudolf, M., Harder, H., Lelieveld, J., Elste, T.,
 Plass-Dülmer, C., Stange, G., and Berresheim, H.: HOx Budgets during HOxComp: a
 Case Study of HOx Chemistry under NOx limited Conditions, J. Geoophys. Res., 117,
 D03307, doi: 10.1029/2011JD017008, 2012a.
 - Fleming, Z. L., Monks, P. S., Rickard, A. R., Bandy, B. J., Brough, N., Green, T. J., Reeves, C. E., and Penkett, S. A.: Seasonal dependence of peroxy radical concentrations at a Northern hemisphere marine boundary layer site during summer and winter: evidence for

- radical activity in winter, Atmos. Chem. Phys., 6, 5415–5433, https://doi.org/10.5194/acp-6-5415-2006, 2006.
 - Geyer, A., Alicke, B., Konrad, S., Schmitz, T., Stutz, J. and Platt, U.: Chemistry and oxidation capacity of the nitrate radical in the continental boundary layer near Berlin, J. Geophys. Res., 106, 8013–8025, 2001.
- Hackenberg, S. C. et al. Potential controls of isoprene in the surface ocean. Glob. Biogeochem. Cycles 31, 644–662, 2017.
 - Hosaynali Beygi, Z., Fischer, H., Harder, H. D., Martinez, M., Sander, R., Williams, J., Brookes, D. M., Monks, P. S., and Lelieveld, J.: Oxidation photochemistry in the Southern Atlantic boundary layer: unexpected deviations of photochemical steady state, Atmos. Chem. Phys., 11, 8497–8513, https://doi.org/10.5194/acp-11-8497-2011, 2011.
- Jenkin, M. E., Young, J. C., and Rickard, A. R.: The MCM v3.3.1 degradation scheme for isoprene, Atmos. Chem. Phys., 15, 11433–11459, https://doi.org/10.5194/acp-15-11433-2015, 2015.
- Jones, C. E., Hornsby, K. E., Sommirava, R., Dunk, R. M., von Glasow, R., McFiggans, G. B., and Carpenter, L. J.: Quantifying the sources and atmospheric impact of marine organic iodine gases, Geophys. Rese. Lett., 37, L18804, doi:10.1029/2010GL043990, 2010.
 - Kanaya, Y., Y. Sadanaga, K. Nakamura, and H. Akimoto (2001), Behavior of OH and HO2 radicals during the Observations at a Remote Island of Okinawa (ORION99) field campaign: 1. Observation using a laser induced fluorescence instrument, J. Geophys. Res., 106, 24,197–24, 208, 2001.
- Lawler, M.J., Finley, B.D., Keene, W.C., Pszenny, A.A.P., Read, K.A., von Glasow, R., Saltzman, E.S.: Pollution-enhanced reactive chlorine chemistry in the eastern tropical Atlantic boundary layer. Geophys. Res. Lett. **36** (2009). doi:10.1029/2008GL036666
- Lee, J.D., McFiggans, G., Allan, J.D., Baker, A.R., Ball, S.M., Benton, A.K., Carpenter, L.J., Commane, R., Finley, B.D., Evans, M., Fuentes, E., Furneaux, K., Goddard, A., Good, N., Hamilton, J.F., Heard, D.E., Herrmann, H., Hollingsworth, A., Hopkins, J.R., Ingham, T., Irwin, M., Jones, C.E., Jones, R.L., Keene, W.C., Lawler, M.J., Lehmann, S., Lewis, A.C., Long, M.S., Mahajan, A., Methven, J., Moller, S.J., Muller, K., Muller, T., Niedermeier, N., O'Doherty, S., Oetjen, H., Plane, J.M.C., Pszenny, A.A.P., Read, K.A., Saiz-Lopez, A., Saltzman, E.S., Sander, R., von Glasow, R., Whalley, L., Wiedensohler, A., Young, D.: Reactive Halogens in the Marine Boundary Layer (RHaMBLe): the tropical North Atlantic experiments. Atmos Chem Phys 10(3), 1031–1055 (2010)
 - Lewis, A.C., Hopkins, J.R., Carpenter, L.J., Stanton, J., Read, K.A., Pilling, M.J.: Sources and sinks of acetone, methanol, and acetaldehyde in North Atlantic marine air. Atmos Chem Phys 5, 1963–1974, 2005.
- Lewis, A.C., Evans, M.J., Methven, J., Watson, N., Lee, J.D., Hopkins, J.R., Purvis, R.M., Arnold, S.R., McQuaid, J.B., Whalley, L.K., Pilling, M.J., Heard, D.E., Monks, P.S.,

- Parker, A.E., Reeves, C.E., Oram, D.E., Mills, G., Bandy, B.J., Stewart, D., Coe, H., Williams, P., Crosier, J.: Chemical composition observed over the mid-Atlantic and the detection of pollution signatures far from source regions. J. Geophys. Res. **112**, D10, 2007.
- Liao, J., et al., Observations of inorganic bromine (HOBr, BrO, and Br2) speciation at Barrow, Alaska, in spring, J. Geophys. Res., 117, D00R16, doi:10.1029/2011JD016641, 2009.

725

730

- Madronich, S. and S. Flocke, The role of solar radiation in atmospheric chemistry, in Handbook of Environmental Chemistry (P. Boule, ed.), Springer-Verlag, Heidelberg, pp. 1-26, 1998.
 - Mahajan, A. S., Plane, J. M. C., Oetjen, H., Mendes, L., Saunders, R. W., Saiz-Lopez, A., Jones, C. E., Carpenter, L. J., and McFiggans, G. B.: Measurement and modelling of tropospheric reactive halogen species over the tropical Atlantic Ocean, Atmos. Chem. Phys., 10, 4611–4624, https://doi.org/10.5194/acp-10-4611-2010, 2010.
- Mao, J.,X. Ren, S. Chen, W.H. Brune, Z. Chen, M. Martinez, H. Harder, B. Lefer, B. Rappenglück, J. Flynn, M. Leuchner, Atmospheric oxidation capacity in the summer of Houston 2006: comparison with summer measurements in other metropolitan studies, Atmos. Environ., 44 (33), 4107, 10.1016/j.atmosenv.2009.01.013, 2010.
- Matsunaga, S., Mochida, M., Saito, T. & Kawamura, K. In situ measurement of isoprene in the marine air and surface seawater from the western North Pacific. Atmos. Environ. 36, 6051–6057 (2002).
 - MERRA-2 data are available at <u>MDISC</u>, managed by the NASA Goddard Earth Sciences (GES) Data and Information Services Center (DISC), https://giovanni.gsfc.nasa.gov/giovanni/. Last visited: June 20, 2021.
- Meusel, H., Kuhn, U., Reiffs, A., Mallik, C., Harder, H., Martinez, M., Schuladen, J., Bohn, B., Parchatka, U., Crowley, J. N., Fischer, H., Tomsche, L., Novelli, A., Hoffmann, T., Janssen, R. H. H., Hartogensis, O., Pikridas, M., Vrekoussis, M., Bourtsoukidis, E., Weber, B., Lelieveld, J., Williams, J., Pöschl, U., Cheng, Y., and Su, H.: Daytime formation of nitrous acid at a coastal remote site in Cyprus indicating a common ground source of atmospheric HONO and NO, Atmos. Chem. Phys., 16, 14475–14493, https://doi.org/10.5194/acp-16-14475-2016, 2016.
 - Miyazaki, Y., Coburn, S., Ono, K., Ho, D. T., Pierce, R. B., Kawamura, K., and Volkamer, R.: Contribution of dissolved organic matter to submicron water-soluble organic aerosols in the marine boundary layer over the eastern equatorial Pacific, Atmos. Chem. Phys., 16, 7695–7707, https://doi.org/10.5194/acp-16-7695-2016, 2016.
 - Millet, D.B., Jacob, D.J., Custer, T.G., de Gouw, J.A., Goldstein, A.H., Karl, T., Singh, H.B., Sive, B.C., Talbot, R.W., Warneke, C., Williams, J.: New constraints on terrestrial and oceanic sources of atmospheric methanol. Atmospheric Chemistry & Physics 8(23), 6887–6905 (2008)

- Milne, P. J., Riemer, D. D., Zika, R. G. & Brand, L. E. Measurement of vertical distribution of isoprene in surface seawater, its chemical fate, and its emission from several phytoplankton monocultures. Mar. Chem. 48, 237–244 (1995).
- Monks, P. S., L. J. Carpenter, and S. A. Penkett (1996), Night-time peroxy radical chemistry in the remote marine boundary later over the Southern Ocean, Geophys. Res. Lett., 23, 535–538.
 - Monks, P. S., L. J. Carpenter, S. A. Penkett, G. P. Ayers, R. W. Gillett, I. E. Galbally, and C. P. Meyer, Fundamental ozone photochemistry in the remote marine boundary layer: The SOAPEX experiment, measurement and theory, Atmos. Environ., 32, 3647–3664, 1998.
- Monks, P.S., Salisbury, G., Holland, G., Penkett, S.A., Ayers, G.P.: A seasonal comparison of ozone photochemistry in the remote marine boundary layer. Atmos. Environ. **34**(16), 2547–2561 (2000)
 - Mungall, E. L., et al. (2017), Microlayer source of oxygenated volatile organic compounds in the summertime marine Arctic boundary layer, Proc. Natl. Acad. Sci. U.S.A., 114, 6203–6208, doi:10.1073/pnas.1620571114, 2017.
- NOAA-GMD: https://www.esrl.noaa.gov/gmd/webdata/ccgg/trends/ch4/ch4_mm_gl.txt, last accessed: 09/26/2021.

780

- Penkett, S. A., Monks, P. S., Carpenter, L. J., Clemitshaw, K. C., Ayers, G. P., Gillett, R. W., Galbally, I. E., and Meyer, C. P.: Relationships between ozone photolysis rates and peroxy radical concentrations in clean marine air over the Southern Ocean, J. Geophys. Res.-Atmos., 102, 12805–12817, 1997.
- Pfannerstill, E. Y., Wang, N., Edtbauer, A., Bourtsoukidis, E., Crowley, J. N., Dienhart, D., Eger, P. G., Ernle, L., Fischer, H., Hottmann, B., Paris, J.-D., Stönner, C., Tadic, I., Walter, D., Lelieveld, J., and Williams, J.: Shipborne measurements of total OH reactivity around the Arabian Peninsula and its role in ozone chemistry, Atmos. Chem. Phys., 19, 11501–11523, https://doi.org/10.5194/acp-19-11501-2019, 2019.
- Ranjithkumar, A., Gordon, H., Williamson, C., Rollins, A., Pringle, K., Kupc, A., Abraham, N. L., Brock, C., and Carslaw, K.: Constraints on global aerosol number concentration, SO₂ and condensation sink in UKESM1 using ATom measurements, Atmos. Chem. Phys., 21, 4979–5014, https://doi.org/10.5194/acp-21-4979-2021, 2021.
- Read, KA, Mahajan, AS, Carpenter, LJ, Evans, MJ, Faria, BVE, Heard, DE, Hopkins, JR, Lee, JD, Moller, SJ, Lewis, AC, Mendes, L, McQuaid, JB, Oetjen, H, Saiz-Lopez, A, Pilling, MJ & Plane, JMC.: Extensive halogen-mediated ozone destruction over the tropical Atlantic Ocean', *Nature*, vol. 453, no. 7199, pp. 1232-1235. https://doi.org/10.1038/nature07035, 2008.
- Read, K.A., Lee, J.D., Lewis, A.C., Moller, S.J., Mendes, L., Carpenter, L.J.: Intra-annual cycles of NMVOC in the tropical marine boundary layer and their use for interpreting seasonal variability in CO. J. Geophys. Res. **114** (2009). doi:10.1029/2009jd011879
- Romer, P. S.; Wooldridge, P. J.; Crounse, J. D.; Kim, M. J.; Wennberg, P. O.; Dibb, J. E.; Scheuer, E.; Blake, D. R.; Meinardi, S.; Brosius, A. L.; Thames, A. B.; Miller, D. O.; Brune, W. H.; Hall, S. R.; Ryerson, T. B.; Cohen, R. C. Constraints on Aerosol Nitrate

- Photolysis as a Potential Source of HONO and NOx. Environ. Sci. Technol. 2018, 52, 13738–13746.
- Pilling, M. J., 2008: Simulating atmospheric gas-phase chemistry: Uncertainties and mechanism reduction problems. Simulation and Assessment of Chemical Processes, I. Barnes and M. M. Kharytonov, Eds., Springer Science, 83–93.
 - Saiz-Lopez, A., J. M. C. Plane, and J. A. Shillito, Bromine oxide in the mid-latitude marine boundary layer, Geophys. Res. Lett., 31, L03111, doi:10.1029/2003GL018956, 2004.
- Sommariva, R., Bloss, W. J., Brough, N., Carslaw, N., Flynn, M., Haggerstone, A.-L., Heard, D. E., Hopkins, J. R., Lee, J. D., Lewis, A. C., McFiggans, G., Monks, P. S., Penkett, S. A., Pilling, M. J., Plane, J. M. C., Read, K. A., Saiz-Lopez, A., Rickard, A. R., and Williams, P. I.: OH and HO₂ chemistry during NAMBLEX: roles of oxygenates, halogen oxides and heterogeneous uptake, Atmos. Chem. Phys., 6, 1135–1153, https://doi.org/10.5194/acp-6-1135-2006, 2006.
- Singh, H., Y. Chen, A. Tabazadeh, Y. Fukui, I. Bey, R. Yantosca, D. Jacob, F. Arnold, K.
 Wohlfrom, E. Atlas, F. Flocke, D. Blake, N. Blake, B. Heikes, J. Snow, R. Talbot, G.
 Gregory, G. Sachse, S. Vay, Kondo, Y.: Distribution and fate of selected oxygenated organic species in the troposphere and lower stratosphere over the Atlantic, J. Geophys. Res., 105(D3), 3795–3805, doi:10.1029/1999JD900779, 2000.
- Sinha, V., Williams, J., Meyerhöfer, M., Riebesell, U., Paulino, A.I., Larsen, A.: Air-sea fluxes of methanol, acetone, acetaldehyde, isoprene and DMS from a Norwegian fjord following a phytoplankton bloom in a mesocosm experiment. Atmos Chem Phys **7**(3), 739–755 (2007)
 - Spataro, F.; Ianniello, A. Sources of atmospheric nitrous acid: State of the science, current research needs, and future prospects. J. Air Waste Manage. Assoc. 2014, 64 (11), 1232–1250, DOI: 10.1080/10962247.2014.952846.

825

830

- Spracklen, D. V., Carslaw, K. S., Merikanto, J., Mann, G. W., Reddington, C. L., Pickering, S., Ogren, J. A., Andrews, E., Baltensperger, U., Weingartner, E., Boy, M., Kulmala, M., Laakso, L., Lihavainen, H., Kivekäs, N., Komppula, M., Mihalopoulos, N., Kouvarakis, G., Jennings, S. G., O'Dowd, C., Birmili, W., Wiedensohler, A., Weller, R., Gras, J., Laj, P., Sellegri, K., Bonn, B., Krejci, R., Laaksonen, A., Hamed, A., Minikin, A., Harrison, R. M., Talbot, R., and Sun, J.: Explaining global surface aerosol number concentrations in terms of primary emissions and particle formation, Atmos. Chem. Phys., 10, 4775–4793, https://doi.org/10.5194/acp-10-4775-2010, 2010.
- Steigvile Byčenkienė, Vidmantas Ulevicius, Nina Prokopčiuk, Dalia Jasinevičienė, Observations of the aerosol particle number concentration in the marine boundary layer over the southeastern Baltic Sea, Oceanologia, 55, 3, 573-597, https://doi.org/10.5697/oc.55-3.573, 2013.
 - Stevens, P. S.: J. H. Mather, W. H. Brune, F. Eisele, D. Tanner, A. Jefferson, C. Cantrell, R. Shetter, S. Sewall, A. Fried, B. Henry, E. Williams, K. Baumann, P. Goldan, W. Kuster: HO2/OH and RO2/HO2 ratios during the Tropospheric OH Photochemistry Experiment: Measurement and theory, J. Geophys. Res., 102, D5, 6379-6391, doi: 10.1029/96JD01704, 1997.
 - Thames, A. B., Brune, W. H., Miller, D. O., Allen, H. M., Apel, E. C., Blake, D. R., Bui, T. P., Commane, R., Crounse, J. D., Daube, B. C., Diskin, G. S., DiGangi, J. P., Elkins, J. W.,

- Hall, S. R., Hanisco, T. F., Hannun, R. A., Hintsa, E., Hornbrook, R. S., Kim, M. J., McKain, K., Moore, F. L., Nicely, J. M., Peischl, J., Ryerson, T. B., St. Clair, J. M., Sweeney, C., Teng, A., Thompson, C. R., Ullmann, K., Wennberg, P. O., and Wolfe, G. M.: Missing OH reactivity in the global marine boundary layer, Atmos. Chem. Phys., 20, 4013–4029, https://doi.org/10.5194/acp-20-4013-2020, 2020.
- Thompson, A. M., Johnson, J. E., Torres, A. L., Bates, T. S., Kelly, K. C., Atlas, E., Greenberg, J. P., Donahue, N. M., Yvon, S. A., Saltzman, E. S., Heikes, B. G., Mosher, B. W., Shashkov, A. A., and Yegorov, V. I.: Ozone observations and a model of marine boundary layer photochemistry during SAGA 3, J. Geophys. Res.-Atmos., 98, 16955–16968, https://doi.org/10.1029/93JD00258, 1993.
- Tran, S. et al. A survey of carbon monoxide and non-methane hydrocarbons in the Arctic Ocean during summer 2010. Biogeosciences 10, 1909–1935 (2013).
 - Vaughan, S., Ingham, T., Whalley, L. K., Stone, D., Evans, M. J., Read, K. A., Lee, J. D., Moller, S. J., Carpenter, L. J., Lewis, A. C., Fleming, Z. L., and Heard, D. E.: Seasonal observations of OH and HO₂ in the remote tropical marine boundary layer, Atmos. Chem. Phys., 12, 2149–2172, https://doi.org/10.5194/acp-12-2149-2012, 2012.
 - Whalley, L.K., Furneaux, K.L., Goddard, A., Lee, J.D., Mahajan, A., Oetjen, H., Read, K.A., Kaaden, N., Carpenter, L.J., Lewis, A.C., Plane, J.M.C., Saltzman, E.S., Wiedensohler, A., Heard, D.E.: The chemistry of OH and HO2 radicals in the boundary layer over the tropical Atlantic Ocean. Atmos Chem Phys 10(4), 1555–1576, 2010.
- Willis, M. D., et al. (2017), Evidence for marine biogenic influence on summertime Arctic aerosol, Geophys. Res. Lett., 44, 6460–6470, doi:10.1002/2017GL073359, 2017.

- Wu YC, Li JL, Wang J, Zhuang GC, Liu XT, Zhang HH, Yang GP. Occurrence, emission and environmental effects of non-methane hydrocarbons in the Yellow Sea and the East China Sea. Environ Pollut. 270, 116305, doi: 10.1016/j.envpol.2020.116305, 2021.
- Xue, C., Ye, C., Kleffmann, J., Zhang, C., Catoire, V., Bao, F., Mellouki, A., Xue, L., Chen, J., Lu, K., Zhao, Y., Liu, H., Guo, Z., and Mu, Y.: Atmospheric Measurements at the Foot and the Summit of Mt. Tai Part I: HONO Formation and Its Role in the Oxidizing Capacity of the Upper Boundary Layer, Atmos. Chem. Phys. Discuss. [preprint], https://doi.org/10.5194/acp-2021-529, in review, 2021.
- Xue, C., Ye, C., Kleffmann, J., Zhang, W., He, X., Liu, P., Zhang, C., Zhao, X., Liu, C., Ma, Z., Liu, J., Wang, J., Lu, K., Catoire, V., Mellouki, A., and Mu, Y.: Atmospheric measurements at Mt. Tai Part II: HONO budget and radical (RO_x + NO₃) chemistry in the lower boundary layer, Atmos. Chem. Phys., 22, 1035–1057, https://doi.org/10.5194/acp-22-1035-2022, 2022.
- Yang, J., R. E. Honrath, M. C. Peterson, D. D. Parrish, and M. Warshawsky: Photostationary state deviation—estimated peroxy radicals and their implications for HOx and ozone photochemistry at a remote northern Atlantic coastal site, J. Geophys. Res., 109, D02312, doi:10.1029/2003JD003983, 2004.

- Ye, C.; Zhang, N.; Gao, H.; Zhou, X. Photolysis of Particulate Nitrate as a Source of HONO and NOx. Environ. Sci. Technol. 2017, 51 (12), 6849–6856.
 - Zhang, S., Sarwar, G., Xing, J., Chu, B., Xue, C., Sarav, A., Ding, D., Zheng, H., Mu, Y., Duan, F., Ma, T., and He, H.: Improving the representation of HONO chemistry in CMAQ and examining its impact on haze over China, Atmos. Chem. Phys. Discuss. [preprint], https://doi.org/10.5194/acp-2021-47, in review, 2021.
- Zhang et al.: Observation and simulation of HOx radicals in an urban area in Shanghai, China, Science of the Total Environment 810 (2022) 152275, https://doi.org/10.1016/j.scitotenv.2021.152275, 2022.
 - Zheng, G., Wang, Y., Wood, R. *et al.* New particle formation in the remote marine boundary layer. *Nat Commun* **12**, 527 (2021). https://doi.org/10.1038/s41467-020-20773-1, 2021.
- Zhou, J., Sato, K., Bai, Y., Fukusaki, Y., Kousa, Y., Ramasamy, S., Takami, A., Yoshino, A., Nakayama, T., Sadanaga, Y., Nakashima, Y., Li, J., Murano, K., Kohno, N., Sakamoto, Y., and Kajii, Y.: Kinetics and impacting factors of HO₂ uptake onto submicron atmospheric aerosols during the 2019 Air QUAlity Study (AQUAS) in Yokohama, Japan , Atmos. Chem. Phys., 21, 12243–12260, https://doi.org/10.5194/acp-21-12243-2021,
 2021.
 - Zhou, S., Gonzalez, L., Leithead, A., Finewax, Z., Thalman, R., Vlasenko, A., Vagle, S., Miller, L. A., Li, S.-M., Bureekul, S., Furutani, H., Uematsu, M., Volkamer, R., and Abbatt, J.: Formation of gas-phase carbonyls from heterogeneous oxidation of polyunsaturated fatty acids at the air—water interface and of the sea surface microlayer, Atmos. Chem. Phys., 14, 1371–1384, https://doi.org/10.5194/acp-14-1371-2014, 2014.
 - Zhou, X. L.; Gao, H. L.; He, Y.; Huang, G.; Bertman, S. B.; Civerolo, K.; Schwab, J., Nitric acid photolysis on surfaces in low- NOx environments: Significant atmospheric implications. Geophys. Res. Lett. 2003, 30, (23).n/a
- Zhou, X.; Zhang, N.; TerAvest, M.; Tang, D.; Hou, J.; Bertman, S.; Alaghmand, M.; Shepson, P. B.; Carroll, M. A.; Griffith, S. Nitric acid photolysis on forest canopy surface as a source for tropospheric nitrous acid. Nat. Geosci. 2011, 4 (7), 440–443.

905

Zhu, Y., Wang, Y., Zhou, X., Elshorbany, Y.F., Ye, C., Hayden, M., Peters, A.J., 2022. An investigation into the chemistry of HONO in the marine boundary layer at Tudor Hill Marine Atmospheric Observatory in Bermuda. Atmos. Chem. Phys. 22, 6327–6346. https://doi.org/10.5194/acp-22-6327-2022.

Highlights

- Explicit analysis of the radical budget in the MBL
- Inefficient recycling of RO₂/HO₂ to OH, more apparent in spring compared to summer.
- Results indicate a possible role of OVOCs from marine sources.
- Halogen monoxides were found to decrease HO_2 by $\sim 15\%$ with a marginal impact on OH.

Declaration of Interest

The authors declare that they have no known competing financial interests or personal relationships that could have appeared to influence the work reported in this paper.